The Ontong Java Plateau

Clive R. Neal[1], John J. Mahoney[2], Loren W. Kroenke[2], Robert A. Duncan[3], and Michael G. Petterson[4]

The Alaska-size Ontong Java Plateau (OJP) in the southwest Pacific is the largest of the world's large igneous provinces and formed entirely in an oceanic environment. Limited sampling of the upper levels of basaltic basement reveals strongly bimodal ages of ≈122 Ma and ≈90 Ma. Geochemical signatures indicate two isotopically distinct, ocean-island-like mantle-source types for the 122 Ma basalts and that the 90 Ma source was almost identical to one of the 122 Ma sources, strongly suggesting that a single mantle plume caused both eruptive events. In the 125–90 Ma period, the OJP appears to have been located near the Pacific Plate Euler poles and thus moved little relative to a postulated hotspot at about 42°S, 159°W; the early phase of emplacement probably also occurred near a spreading center, but substantial volumes were emplaced off-axis. The eastern lobe of the plateau appears to have been rifted shortly after 90 Ma. Incompatible and major element data are consistent with 20–30% polybaric partial melting of a peridotite source, beginning in the garnet stability field and continuing in the spinel field. Most existing basaltic basement samples appear to have experienced 30–45% of crystal fractionation; the resulting cumulates would be wehrlitic to pyroxenitic in composition, with an average density of ≈3.25 g cm^{-3}. We conclude that these cumulates form much of the plateau's high velocity (≈7.6 km s^{-1}) basal crustal layer. The relatively high density of this layer appears to have prevented emergence of much of the OJP above sea level despite a total crustal thickness exceeding 30 km. Although the deepest levels of the crust could be eclogitized (further increasing density), post-emplacement subsidence of the plateau has probably been tempered by the presence of a roughly 85-km-thick melt-depleted mantle root with a relatively low density (≤3.25 g cm^{-3}) for mantle material. Estimates of partial melting deduced from the apparent thickness of the mantle root imply that the OJP formed by 17–31% partial melting, in excellent agreement with geochemical modeling.

[1]Department of Civil Engineering and Geological Sciences, University of Notre Dame, Notre Dame, Indiana
[2]School of Ocean and Earth Science and Technology, University of Hawaii at Manoa, Honolulu, Hawaii
[3]College of Oceanic and Atmospheric Sciences, Oregon State University, Corvallis, Oregon
[4]British Geological Survey, Muchison House, West Mains Road, Edinburgh, United Kingdom

Large Igneous Provinces: Continental, Oceanic, and Planetary Flood Volcanism
Geophysical Monograph 100

1. INTRODUCTION

Oceanic plateaus are now generally recognized as the counterparts of continental flood basalts and thick volcanic sequences found at many passive plate margins. Collectively, such areas have been termed large igneous provinces or LIPs [e.g., *Coffin and Eldholm*, 1991]. Since the mid-1980s, a consensus has grown among geochemists and geodynamicists that most oceanic plateaus are created at hotspots; more recently, the larger plateaus have been ascribed to the initial "plume-head" stage of hotspot development [e.g., *Richards et al.*, 1991; *Saunders et al.*, 1992; *Kent et al.*, 1992]. Many laboratory experiments, along with numerical modeling, suggest that mantle plume

initiation caused by a temperature instability at a boundary layer results in a large, inflated "plume-head" trailed by a narrow feeder conduit or "tail" [e.g., *Whitehead and Luther*, 1975; *Olson and Singer*, 1985; *Griffiths and Campbell*, 1990; *Neavel and Johnson*, 1991]. In plume-head models, emplacement of the LIP occurs in a geologically short period of only a few million years or less [e.g., *Richards et al.*, 1989]. This is a consequence of extensive decompressional melting when the rising plume head, with temperatures argued to average up to 300°C above those of ambient upper mantle, approaches and spreads out at the base of the lithosphere, where it may reach a diameter of 2000 km or more [e.g., *Campbell and Griffiths*, 1990; *Hill et al.*, 1992; *Ribe et al.*, 1995; *Kincaid et al.*, 1996]. For the largest plateaus, the enormous size of the source required suggests an origin of the plume in the lower mantle, possibly at the core-mantle boundary; a plume head originating at the 660-km mantle discontinuity, for example, would not reach sufficient size to account for the volume of magma required to generate the larger LIPs [e.g., *Coffin and Eldholm*, 1993].

Several major oceanic plateaus are located in the Pacific Ocean basin, including Hess Rise, Shatsky Rise, the Mid-Pacific Mountains, the Manihiki Plateau, and the world's largest, the Ontong Java Plateau (OJP) (Figure 1). Unlike their continental and continental-margin analogs, plateaus formed in intraoceanic settings offer a means of studying LIP sources and structure and testing models of LIP origin without the often considerable complications caused by the presence of continental lithosphere. Unfortunately, the crustal basements of oceanic plateaus remain very poorly sampled, in general, because they are largely submerged and buried beneath thick covers of marine sediments. Of the plateaus in the Pacific, the OJP is by far the best-sampled, with basement penetrations at Deep Sea Drilling Project (DSDP) Site 289 (9 m), and Ocean Drilling Program (ODP) sites 803 (26 m) and 807 (149 m). Moreover, tectonically uplifted portions of OJP basement are exposed above sea level in the eastern Solomon Islands of Santa Isabel, Ramos, Malaita, and Ulawa (Figures 2 and 3). Some of the thickest exposures on these islands recently have been sampled in detail; studies are still underway, but the results now available provide a much better, though often surprising, picture of the OJP than was available only a few years ago. This paper presents a review of geochemical, geochronological, and geophysical knowledge about the plateau and additionally reports new results of a detailed geochemical investigation of the top 2–3 km of volcanic basement exposed on the island of Malaita. Particular attention is given to the origin and effect of "hidden" cumulates in the crust of the plateau.

2. PHYSICAL FEATURES AND GROSS STRUCTURE OF THE OJP

The Alaska-size OJP covers an area of more than 1.5×10^6 km^2 and consists of two parts: the main, or high, plateau in the west and north and the eastern lobe or salient (Figure 2). The plateau surface rises to depths of ≈1700 m in the central region of the high plateau but lies generally between 2 and 3 km depth. The OJP is bounded to the northwest by the Lyra Basin, to the north by the East Mariana Basin, by the Nauru Basin to the northeast and the Ellice Basin to the southeast (Figure 1). Along its southern and southwestern boundaries the OJP has collided with the Solomon Islands arc and it now lies at the junction between the Pacific and Australian plates, extending eastward to the Vitiaz arc-trench system.

Although much of the surface is relatively smooth, the top of the plateau is punctuated by several sizable seamounts, including Ontong Java atoll (the largest atoll in the world), and physiography around the margins of the plateau is complicated [e.g., *Kroenke*, 1972; *Berger et al.*, 1993]. In many areas, the basement crust is covered with pelagic sediments >1 km thick, which are thickest where the plateau is at its most shallow [e.g., *Mayer et al.*, 1991]. Rough basement topography on the margins of the OJP has been interpreted as extensional horst and graben structures that predate much of the sediment cover [e.g., *Ewing et al.*, 1968; *Kroenke et al.*, 1971; *Kroenke*, 1972; *Berger and Johnson*, 1976; *Hagen et al.*, 1993].

Crustal thickness on much of the high plateau is considerable even in comparison to other plateaus. Non-seismic methods (e.g., gravity data) provide a lower limit of 25 km [*Cooper et al.*, 1986; *Sandwell and Renkin*, 1988], whereas seismic and combined seismic-gravity evidence indicates crustal thicknesses in the 30–43 km range, with an estimated average around 36 km [e.g., *Furumoto et al.*, 1970, 1976; *Murauchi et al.*, 1973; *Hussong et al.*, 1979; *Miura et al.*, 1996; *Richardson and Okal*, 1996; *Gladczenko et al.*, 1997]. A 36-km thickness translates to a volume of $> 5 \times 10^7$ km^3 [*Mahoney*, 1987; *Coffin and Eldholm*, 1993]. The maximum extent of OJP-related volcanism may be even greater, as the Early Cretaceous lavas filling the Nauru Basin to the northeast of the OJP and similar lavas in the East Mariana and Pigafetta basins to the north have been proposed to be closely related to the OJP [e.g., *Castillo et al.*, 1991, 1994; *Gladczenko et al.*, 1997 and references therein]. Indeed, by analogy with some continental flood basalt provinces [see *Ernst and Buchan*, this volume], the lavas in these basins might reflect one or more giant radiating dike swarms associated with emplacement of the OJP.

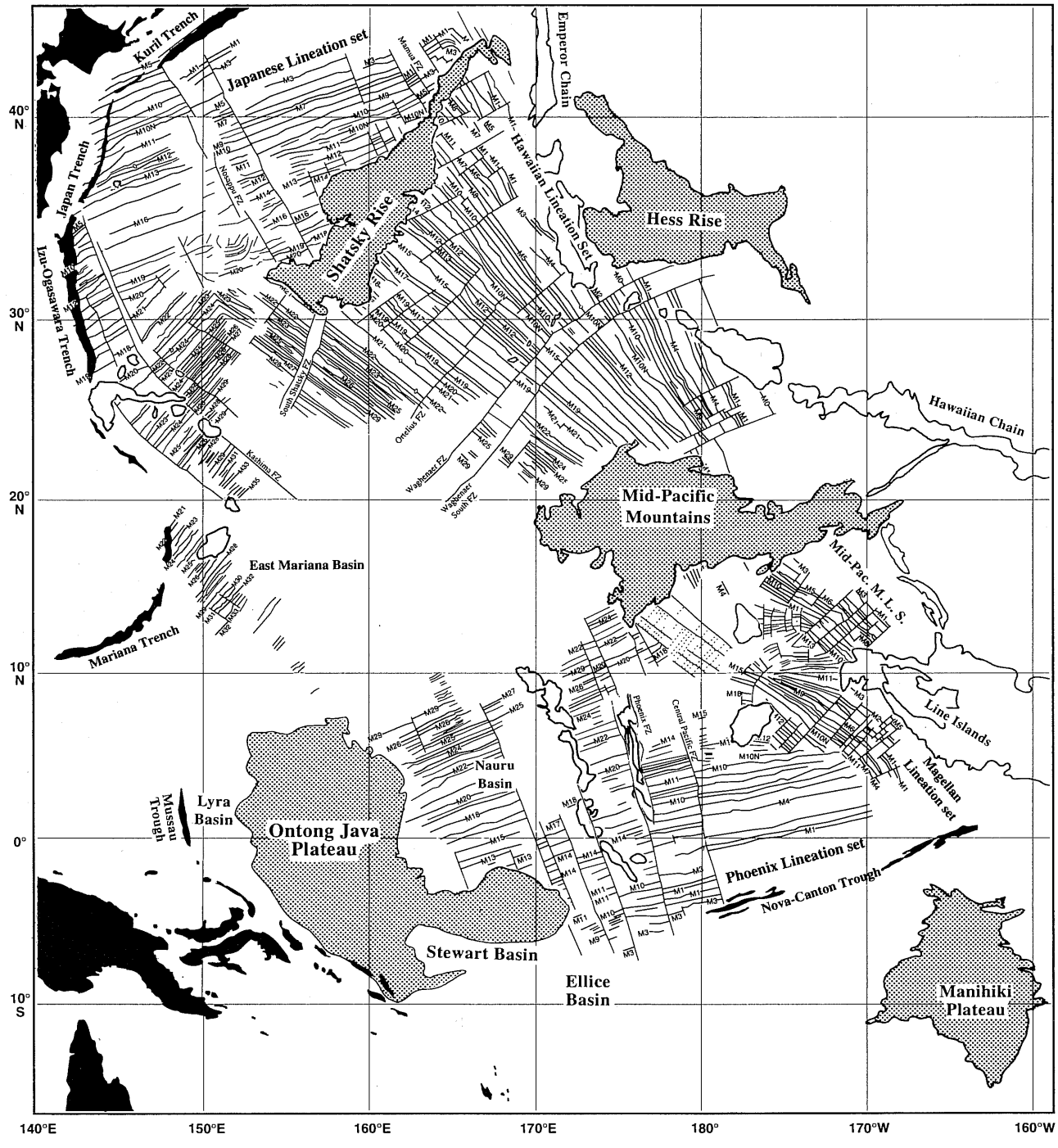

Figure 1. Map of the west-central Pacific showing locations of principal oceanic plateaus (shaded) and magnetic anomaly lineations [after *Nakanishi et al.*, 1992].

Results of recently completed seismic studies of crustal structure have, as yet, been presented only in abstract form [e.g., *Miura et al.*, 1996]. Nevertheless, a simple crustal model can be constructed from pre-1995 seismic refraction and sonobuoy wide-angle reflection/refraction measurements, despite the limitations of the data (Figure 2). Broadly, the OJP appears to have a crustal seismic structure resembling that of normal Pacific oceanic crust,

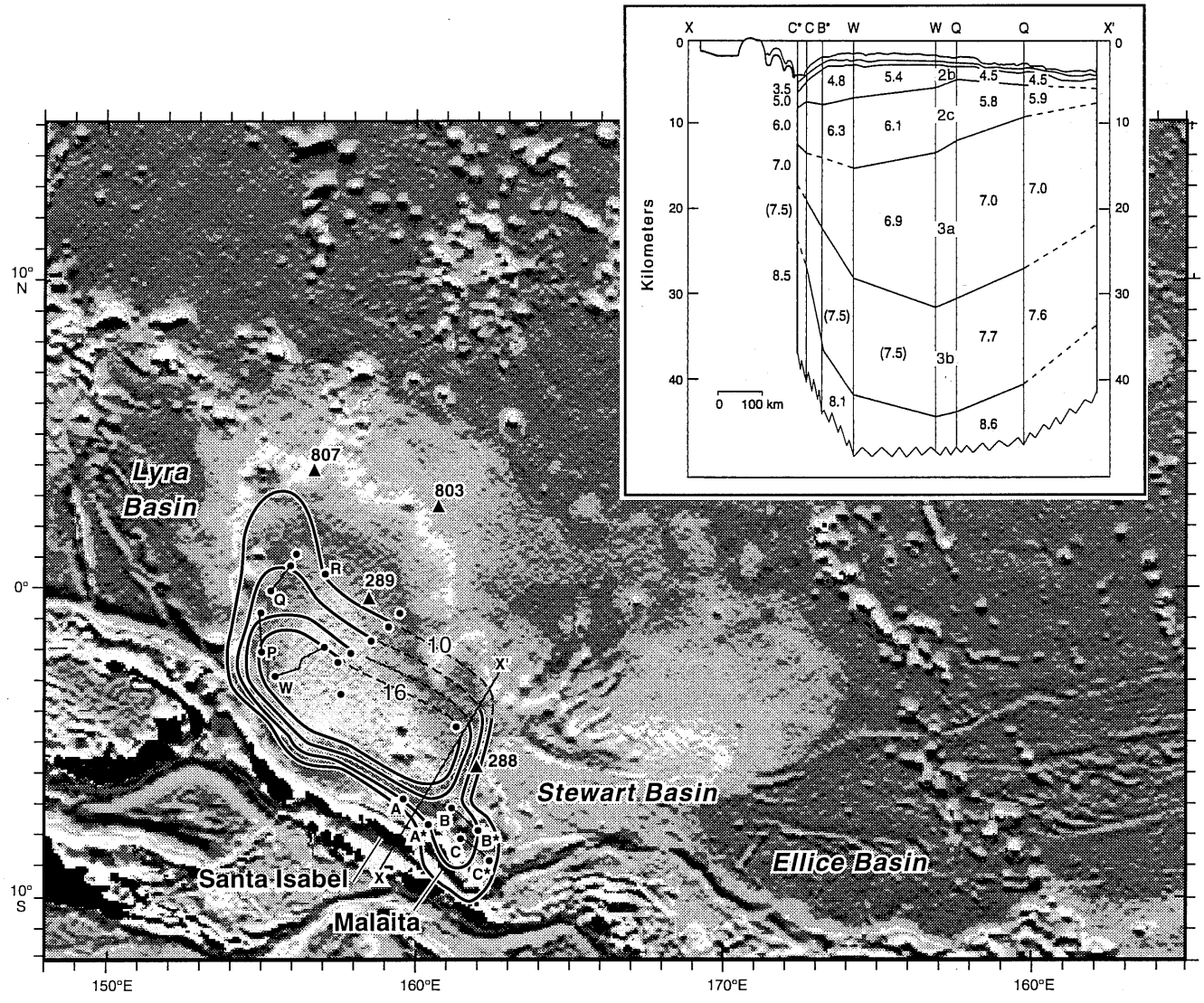

Figure 2. E-topo 5 bathymetric map of the western equatorial Pacific Basin (centered on the OJP and Nauru Basin, shaded by satellite-derived gravity fabric illuminated from the north [after *Smith and Sandwell*, 1995a,b]). The locations of drill sites 807, 803, 289, and 288 (the latter did not reach basement) are shown as triangles. Contours represent the depth to the top of Layer 3A in the high plateau (contour interval = 2 km). Deep crustal seismic refraction lines are labeled A-A*, B-B*, and C-C* [from *Furumoto et al.*, 1970] and P, Q, and R [from *Furumoto et al.*, 1976]. Sonobuoy refraction lines [from *Hussong et al.*, 1979] are represented by isolated dots. Inset is composite crustal cross-section X-X′. P-wave velocities (in km s^{-1}) are from *Furumoto et al.* [1970, 1976]; velocities in parentheses have been inserted following *Hussong et al.* [1979].

but each layer is abnormally thickened by up to a factor of five [*Hussong et al.*, 1979]. Figure 2 shows a composite section (XX′) across the high plateau which depicts a thick crustal lens, more than 40 km thick where it underpins the center of the OJP. Such a crustal configuration is consistent with a structure-contour map showing the top of Layer 3A on the high plateau also presented in Figure 2. This is based, in part, on data from the refraction surveys of *Furumoto et al.* [1970, 1976], but uses only the most reliable, upper crustal data, all from first arrivals; it also uses the later sonobuoy measurements summarized by *Hussong et al.* [1979], which showed Layer 2B velocities to be remarkably uniform. The upper crustal section includes the water column, sediments (containing some

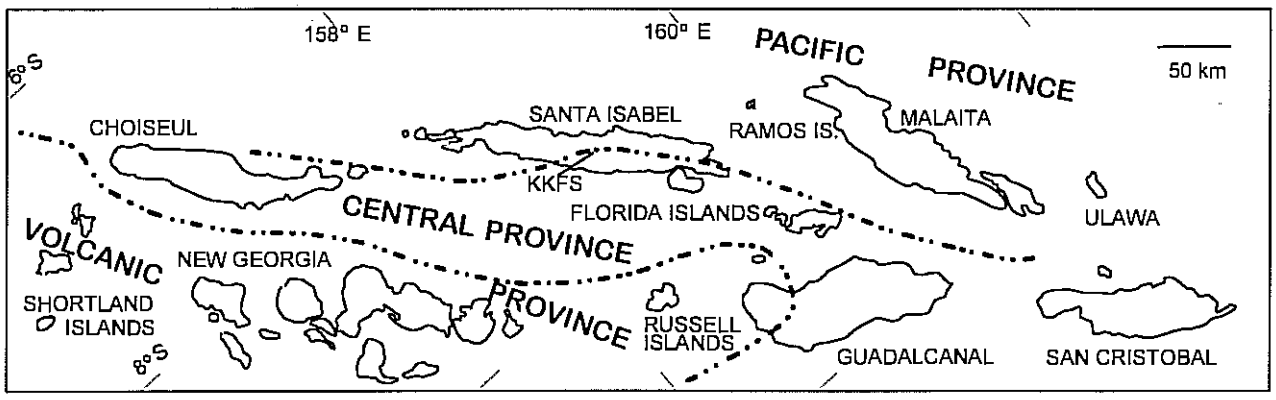

Figure 3. Division of the Solomon Islands chain into geologically distinct regions of the Pacific, Volcanic, and Central Provinces [e.g., *Coleman*, 1966, 1976; *Coleman and Packham*, 1976].

high-velocity horizons), Layer 2B (composed of dense, high velocity basalts), and Layer 2C (dolerites?). Depths to the top of Layer 3A (with P-wave velocities in the 6.9-7.0 km s^{-1} range, appropriate for high-level gabbros or possibly mafic granulites [e.g., *Rudnick and Jackson*, 1995]) range from less than 10 km around the plateau's edges to more than 16 km in a broad central region of the high plateau. The general shape is an elongate, ESE-WNW-trending depression, in much of which Layer 2 is over 12 km thick.

On the central and western parts of the high plateau, Layer 3B velocities are established to be rather high at 7.6–7.7 km s^{-1} (Figure 2). This range is appropriate for granular gabbros [*Schaefer and Neal*, 1994; *Farnetani et al.*, 1995, 1996] or garnet granulites [*Nixon and Coleman*, 1978], although *Houtz and Ewing* [1976] considered such velocities to be compatible with deep oceanic basalts or serpentinized peridotites. High sub-Moho velocities of 8.4–8.6 km s^{-1}, appropriate for eclogite [*Neal and Taylor*, 1989; *Rudnick and Jackson*, 1995; *Saunders et al.*, 1996] were detected in the northwest and southwest portions of the plateau.

3. TECTONIC SETTING OF OJP EMPLACEMENT

The original plate tectonic setting of the OJP is open to some question because well-defined magnetic anomaly lineations do not appear to be present on the plateau. Possible spreading-ridge or fracture-zone fabric is subdued and difficult to interpret unambiguously, and most pre-OJP crust to the west and south of the plateau has been subducted. However, block-faulting structures along the eastern margin of the high plateau were interpreted by *Andrews and Packham* [1975] and *Hussong et al.* [1979] to be parts of fracture zones trending roughly NNE. This feature, together with the OJP's crustal velocity structure, possible very low-amplitude magnetic anomalies across the northern half of the high plateau, and the very sparse age data for plateau basement lavas available at the time, led *Hussong et al.* [1979] to propose an origin of the OJP at an unusually active, WNW-trending, slow-spreading ridge over a period of several tens of millions of years. An age progression across the plateau was implicit in this interpretation. Variations on this hypothesis proposed that the OJP was formed at a migrating triple junction or transform during a period of ridge jumping and heavy volcanism [*Winterer*, 1976; *Hilde et al.*, 1977; *Taylor*, 1978]; however, explanations for why volcanism was heavy were lacking. On the basis of preliminary isotopic and elemental data, together with the geophysical evidence, *Mahoney* [1987] proposed that the OJP was formed by a large ridge-centered or near-ridge plume, and discussed the possibility that this plume was the early Louisville hotspot (now located at ≈53°S [*Wessel and Kroenke*, 1997]).

Subsequent major and trace element data for basement lavas from drill sites on the OJP and from outcrops in Malaita and Santa Isabel (summarized below) were found to be consistent with the plateau having formed in the vicinity of a spreading center (or at least on thin lithosphere) by high fractions of partial melting [*Mahoney et al.*, 1993; *Tejada et al.*, 1996a]. *Tarduno et al.* [1991], *Richards et al.* [1991], and *Mahoney and Spencer* [1991] all favored the Louisville hotspot as the plume involved in the origin of the OJP; however, following *Richards et al.* [1989], they attributed the plateau to a cataclysmic outpouring of magma associated with the initial, plume-head stage of the hotspot, probably in the early Aptian. *Mahoney and Spencer* [1991] argued that, even if not initially surfacing near a spreading axis, plume heads

would tend to attract ridges because of their expected control on rift propagation. Recently, *Winterer and Nakanishi* [1995] also inferred a near-ridge plume origin for the OJP; however, they interpreted bathymetry and the fabric in the new satellite-derived gravity map of *Smith and Sandwell* [1995a,b] to indicate an orientation of fracture zones and spreading axis nearly perpendicular to that suggested by *Hussong et al.* [1979].

The plateau geometry inferred by *Winterer and Nakanishi* [1995] appears difficult to reconcile with the nearby ENE-WSW M-series Nauru magnetic lineations on the east side of the OJP [e.g., *Nakanishi et al.*, 1992] (Figure 1). Moreover, *Taylor* [1978] reported M-series magnetic anomaly lineations in the nearby Lyra Basin on the west side of the OJP roughly paralleling those in the Nauru Basin on the east. A more recent aeromagnetic survey in the Lyra Basin also revealed roughly ENE-WSW-oriented M-series magnetic anomaly lineations (B. Taylor, personal communication, 1995). Our interpretation of the combined bathymetry and gravity map of *Smith and Sandwell* [1995a,b] is that the data are consistent with a NNE-trending fracture-zone fabric on the high plateau.

Rather than providing evidence for either a single, brief, cataclysmic emplacement event or a basement age progression, recent ^{40}Ar-^{39}Ar ages for OJP basement lavas yield an intriguing, strongly bimodal distribution. The ages of lavas from Sites 289, 807, and 803 on the high plateau, as well as for basement lavas from Malaita, Ramos, and Santa Isabel, suggest that most of the plateau may have formed in two relatively brief episodes, the first at 122±3 Ma, the second at 90±4 Ma (errors indicate total ranges rather than weighted means) [*Mahoney et al.*, 1993; *Tejada et al.*, 1996a,b; *Parkinson et al.*, 1996]. Thus, much of the fabric interpreted from bathymetry and satellite-derived gravity data is likely to represent preexisting oceanic crust covered by widespread plateau-basalt eruptions, consistent with pre-122 Ma, southward-younging M-series magnetic anomaly lineations in the Nauru and Lyra basins. Although a spreading center may well have been present, at least in the 122 Ma phase of eruptions, substantial magmatism must have occurred well beyond the immediate vicinity of a ridge axis. Indeed, available geophysical evidence weakly favors emplacement of most OJP lavas in an off-ridge location [*Coffin and Gahagan*, 1995]. As sampling of the plateau is still very limited, the relative crustal volumes of the ≈122 and ≈90 Ma episodes, and thus emplacement rates, are as yet unclear. However, *Tejada et al.* [1996a,b] and *Kroenke and Mahoney* [1996] suggested that the 122 Ma episode was significantly larger than the 90 Ma event, hypothesizing that the 122 Ma event generally corresponded to the construction of the main, high plateau and that the eastern salient was the main focus of activity at 90 Ma.

4. THE OJP AND CRETACEOUS PLATE MOTIONS

Formation of the larger oceanic plateaus in the Pacific appears to be associated temporally with major changes in Pacific Plate motion. Four such changes appear to have occurred in the Late Jurassic to Early Cretaceous, a time when the plate was relatively small and being guided by the motion of adjoining plates [*Kroenke and Sager*, 1993]. These changes, at about 140, 125, 110, and 100 Ma, appear to have occurred near the times of formation of the Shatsky Rise, OJP (early event) and Manihiki Plateau, western and northern Hess Rise, and central Hess Rise, respectively, along or near the divergent boundaries of the Pacific Plate [*Kroenke and Sager*, 1993]. The most pronounced change in motion occurred at ≈125 Ma, between magnetic anomalies M1 and M0 near the Barremian-Aptian boundary [e.g., *Steiner and Wallick*, 1992], and was probably concomitant with the cessation of southwestward subduction beneath northeastern Gondwana and the beginning of northwestward subduction beneath Eurasia. This event can be noted, for example, in the reversal in magnetic anomaly lineation pattern from M3-M1 to M1-M3 east of the OJP near the west end of the Nova-Canton Trough (Figure 1; see also *Nakanishi and Winterer* [1996]). Associated with this change was the formation of a large portion of the OJP (i.e., the 122±3 Ma event) and the Manihiki Plateau (R. A. Duncan, unpubl. data, 1993). Unfortunately, existing data do not allow resolution of whether OJP eruptions followed or at least partly preceded the change. Indeed, ^{40}Ar-^{39}Ar dates for OJP lavas provide some of the best estimates of the minimum age of magnetic reversal M0 and the Barremian-Aptian boundary [*Pringle et al.*, 1992; *Mahoney et al.*, 1993].

Rough pre-100 Ma Pacific Plate motions can now be determined back to ≈145 Ma, using (1) the probable age progression along the Shatsky Rise estimated by *Sager and Han* [1993]; (2) paleomagnetic evidence of a change from a southward to a northward component of plate motion at ≈125 Ma [*Steiner and Wallick*, 1992] and limited latitudinal movement until about 90 Ma at the latitude of the Mid-Pacific Mountains [*Tarduno and Sager*, 1995]; (3) recently mapped magnetic anomaly lineations in the west-central Pacific [*Nakanishi et al.*, 1992]; (4) charts of central and western Pacific seamounts [*Mammerickx and Smith*, 1985]; and (5) the new satellite-derived gravity maps of *Smith and Sandwell* [1995a,b]. Figure 4 (bottom) shows the site of the OJP at approximately 125 Ma on the Pacific Plate, far from continental influences, centered at

about 42°S, 159°W. From about 125 Ma until approximately 100 Ma the OJP appears to have been positioned very close to the Pacific Plate Euler poles, and thus moved relatively little. At approximately 100 Ma, plate motion changed from a northwestward to a more northward trajectory, and from about 100 Ma to approximately 85 Ma the OJP moved steadily northward with the plate [*Yan and Kroenke*, 1993]. The plate reconstruction model of *Yan and Kroenke* [1993] shows that at 90 Ma, the age of the second major eruptive event, the eastern margin of the OJP passes approximately over the position occupied by the central high plateau at 125 Ma (Figure 4, middle).

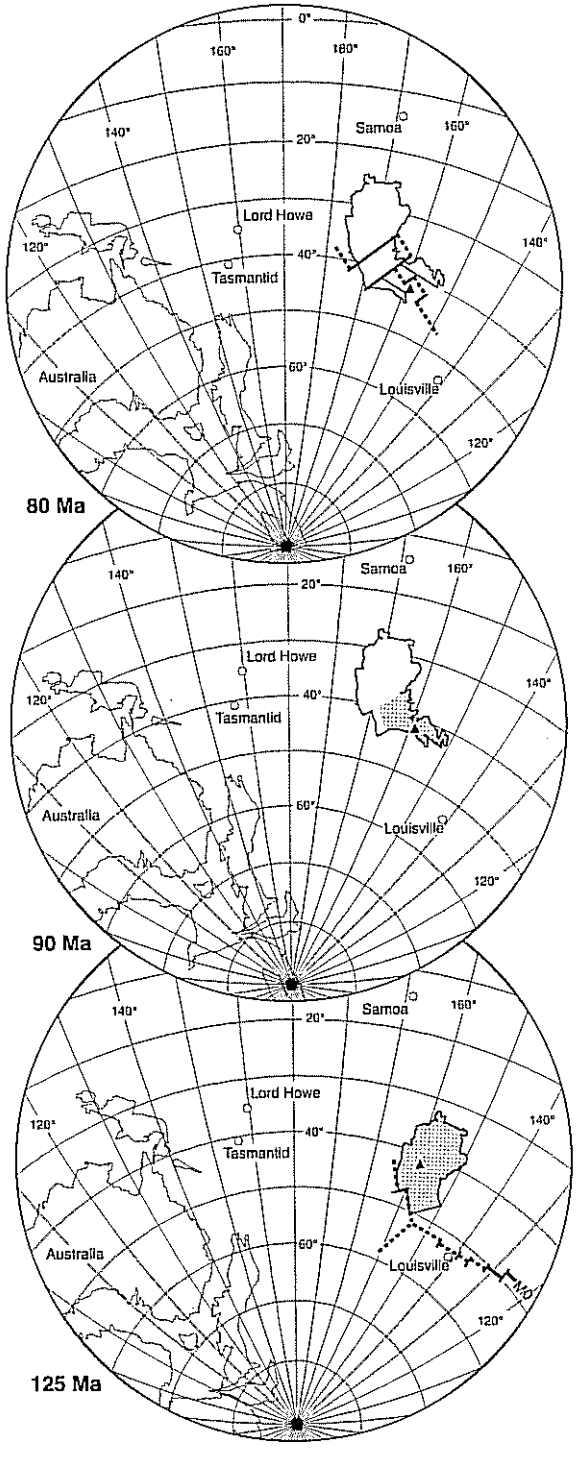

The location of the plateau in the 125 Ma reconstruction of Figure 4 is at least roughly consistent with paleomagnetic data for basement and basal sediments at Site 289, which yield a paleolatitude of 30–35°S [*Hammond et al.*, 1975]; a similar paleolatitude is indicated by basement lavas at Site 807, although basement there may have been tilted around the time of emplacement [*Mayer and Tarduno*, 1993]. No hotspot is known to exist today in the vicinity of the triangle shown in Figure 4, but this area is one of the least surveyed in the world's oceans. This location is ≈1800 km distant from the Louisville hotspot, which, as noted above, has been suggested by several workers to be linked to the OJP and which has a well-marked seamount trail (the Louisville Ridge or Seamount Chain) going back to ≈70 Ma. Older portions of the Louisville hotspot trail, if they existed, have been destroyed by the Vitiaz-Tonga trench system [cf. *Mahoney and Spencer*, 1991]. To accommodate a Louisville hotspot origin for the OJP, true polar wander of ≈10–15° since 125 Ma must be invoked [e.g., *Mayer and Tarduno*, 1993]. Also, isotopic and elemental data for the 122 and 90 Ma OJP lavas are closely similar to each other, consistent with a single plume being responsible for both eruptive episodes, but they are distinct, particularly in Pb isotopic ratios, from the 0–70 Ma lavas of the Louisville Seamount Chain (see Section 6.3.1). At present, identification of the hotspot associated with the OJP remains elusive.

Between about 90 and 85 Ma, a major change in Australian and Antarctic Plate motions took place as

Figure 4. Bottom: approximate location of the OJP high plateau at 125 Ma. Shading represents postulated extent of 122 Ma volcanism. Several present-day hotspots are shown as circles. The triangle represents the inferred location of the OJP plume center beneath the crest of the high plateau. Heavy lines indicate a possible spreading ridge arrangement (schematic except at the eastern end). Middle: location of the OJP at 90 Ma; note that the eastern lobe of the plateau is now above the inferred plume center. Here, shading represents the postulated region of heaviest 90 Ma volcanism. Top: reconstruction for 80 Ma showing rifting of the eastern lobe (schematic). The 125 Ma reconstruction uses the 125–110 and 110–100 Ma Pacific Plate Euler poles of *Kroenke and Wessel* [1997]; the 90 and 80 Ma reconstructions are after *Yan and Kraenke* [1993].

spreading began in the Tasman Basin and in the Southwest Pacific Basin, south of Campbell Plateau [*Cande et al.*, 1989]. Following the ≈90 Ma eruptive episode on the OJP, post-emplacement rifting and seafloor spreading may have occurred for up to several million years within the plateau's eastern salient, in conjunction with spreading in the Ellice Basin to the east (Figure 4, top). A rifted character is suggested by the recent satellite-derived gravity data of *Smith and Sandwell* [1995a,b], which show that the northern and southern ridges bounding the bathymetric low in the eastern salient resemble conjugate ridges, with slight gravity lows on their southern and northern sides, respectively (Figure 2). A similar rift-margin fabric extends eastward across the adjoining Ellice Basin. Magnetic lineations have been detected in the Ellice Basin trending roughly east-west (D. Handschumacher, unpubl. data) but have not yet been identified; however, *Duncan* [1985] obtained an ^{40}Ar-^{39}Ar date of 82.6±1.2 Ma for a mid-ocean-ridge-type basalt from the eastern end of the Ellice Basin. Note that rifting of the eastern salient and spreading in the Ellice Basin soon after the ≈90 Ma OJP episode could explain why the OJP is not connected physically to a post-plateau chain of seamounts (the "plume-tail" stage of hotspot development).

5. RELATIONSHIP TO THE SOLOMON ISLANDS

Along the plateau's southern and southwestern margins, basement topography reflects faulting and deformation caused by the collision of the OJP with the Solomon Islands arc [e.g., *Kroenke*, 1972; *Kroenke et al.*, 1986, 1991; *Auzende et al.*, 1996]. The OJP arrived at the old Solomon arc during the early Neogene in a "soft" docking without significant deformation, with southwest-directed subduction ending around 27–23 Ma [e.g., *Coleman and Kroenke*, 1981; *Cooper and Taylor*, 1985]. Initiation of northeast-directed subduction beneath the plateau occurred progressively from the ESE because collision of the OJP with the old arc was diachronous. Collision moved WNW along the arc throughout the Neogene as a result of the general westward motion of the OJP, with subduction beginning on the plateau's south side at 10–5 Ma and continuing throughout the Pliocene along the arc [*Mann et al.*, 1996]. Subduction during the quiescent period between 27–23 Ma and 10–5 Ma appears to have been occurring in the Tonga and Trobriand trenches instead. The collision of the Woodlark Basin spreading-ridge complex with the southwest-facing San Cristobal forearc pushed the arc northeastward into the OJP and produced the Malaita Anticlinorium, an extensive fold belt embracing the eastern Solomon islands of Malaita, Ulawa, Ramos, and the northern half of Santa Isabel [*Kroenke*, 1972; *Kroenke et al.*, 1986; *Petterson*, 1995; *Petterson et al.*, 1997]. These islands appear to represent the tops of several-km-thick "tectonic flakes" of OJP crust thrusted onto the old forearc-backarc region, probably during the Pliocene [e.g., *Kroenke*, 1972; *Petterson et al.*, 1997]. Farther south, a large thrust-sheet of OJP crust forms the seafloor south of Malaita [*Auzende et al.*, 1996], possibly extending to and even including part of Makira (San Cristobal) [*Petterson et al.*, 1995; *Birkhold-VanDyke et al.*, 1996].

The Solomon Islands group has been subdivided for several decades into three geological regions or provinces (Figure 3) [e.g., *Coleman*, 1966, 1976; *Hackman*, 1973; *Coleman and Packham*, 1976]. The eastern region, termed the Pacific Province, appears to be an uplifted, overthrusted, largely unmetamorphosed portion of the OJP, as noted above [additional references include *Andrews and Packham*, 1975; *Hughes and Turner*, 1977; *Coleman et al.*, 1978; *Coleman and Kroenke*, 1981; *Ramsay*, 1982; *Hopson*, 1988; *Petterson*, 1995; *Tejada et al.*, 1996a]. Adjacent to the Pacific Province on the southwest is the Central Province, which contains variably metamorphosed Cretaceous and Early Tertiary seafloor and remnants of the northeast-facing arc sequence that grew during the Early to Middle Tertiary above the then southwest-plunging Pacific Plate (prior to the arrival of the OJP from the east). The boundary between the Pacific and Central provinces is generally submerged, but lies above sea level on Santa Isabel, where it forms a fault zone termed the Kaipito-Korighole fault system [e.g., *Hawkins and Barron*, 1991; *Tejada et al.*, 1996a]. Along the southwestern flank of the Central Province is the Volcanic Province, an island arc sequence composed of volcanic and intrusive rocks and active volcanoes; the age of this province appears to be <4 Ma [e.g., *Petterson*, 1995]. Significantly, the plateau appears to be more or less unsubductable [*Cloos*, 1993; *Abbott and Mooney*, 1995]. However, the post-Miocene removal of a portion of the lower OJP between Santa Isabel and Makira is evident from recent seismic surveys [*Mann et al.*, 1996; *Phinney et al.*, 1996; *Cowley et al.*, 1996].

6. GEOCHEMISTRY AND AGE OF BASEMENT

6.1. *Submarine Drillholes*

The only detailed basement stratigraphy for the entire plateau, prior to the recent and ongoing work in Malaita and Santa Isabel, came from the 149-m-thick section of ODP Site 807 and the 26 m section of Site 803 [*Mahoney et al.*, 1993]. At Site 807, the section has been divided into several units (A, C-G), each of which is a packet of low-K, tholeiitic pillow lavas and massive flows, except for Unit

F, which consists of a single 28-m-thick flow, and Unit B which is a 50-cm-thick interlava limestone [*Kroenke et al.*, 1991; *Mahoney et al.*, 1993]. Unit A (46 m thick) is isotopically (Figure 5) and chemically (Figure 6 and Table 1) distinct from Units C-G in having lower $^{206}Pb/^{204}Pb$ (18.3–18.4 vs. 18.6–18.7) and initial ε_{Nd} (+4.8 – +5.4 vs. +5.9 – +6.3), higher initial $^{87}Sr/^{86}Sr$ (0.7040–0.7041 vs. 0.70339–0.70345), and slightly higher ratios of highly incompatible to moderately incompatible elements. Consistent with a plume-head origin, the isotopic values of both groups fall within the range of those for "Dupal-type" hotspot islands (although few present-day islands have values closely similar to those of the OJP lavas). Except for elements especially susceptible to seawater alteration (e.g., Rb, K, Cs), primitive-mantle-normalized incompatible element patterns are quite flat (Figure 6), although some of the most incompatible elements are relatively depleted (e.g., Ba and Th); Li and P are also depleted whereas Mo is relatively enriched (note that rock powders were ground in alumina). Major and trace element compositions suggest both groups reflect high degrees of melting (probably 20–30%, with Units C-G representing slightly higher degrees of melting than Unit A). The single flow sampled at DSDP Site 289 is nearly identical to the Units C-G lavas. Although differing somewhat in major element composition, the Site 803 lavas are closely similar isotopically to the Units C-G basalts, with identical $^{206}Pb/^{204}Pb$ and initial ε_{Nd} and only slightly higher initial $^{87}Sr/^{86}Sr$ (0.7036–0.7037) (Figure 5). Their incompatible element signature is also similar to that of Units C-G, although they are slightly enriched in the more highly incompatible elements (Figure 6 and Table 1).

The ^{40}Ar-^{39}Ar ages for Unit A and Units C-G lavas, as well as the Site 289 basalt, are identical, within errors, at ≈122 Ma [*Mahoney et al.*, 1993]. However, the Site 803 lavas yielded significantly younger ages of ≈90 Ma; sediments above basement at Site 803 could not be used to confirm this age as the site is located in a depression which appears to contain derived sediments [*Kroenke et al.*, 1993; *Mahoney et al.*, 1993; *Sliter and Leckie*, 1993]. Foraminiferal ages of these sediments vary from Barremian to Lower Aptian [*Sliter and Leckie*, 1993].

6.2. *Santa Isabel*

The ≈90 Ma event was confirmed by ^{40}Ar-^{39}Ar results for the tholeiitic Sigana Basalts, which form the basement of the northern portion (Pacific Province) of Santa Isabel and Ramos Island. Both the ≈122 Ma and ≈90 Ma groups are present, with the 90 Ma lavas being particularly abundant in the middle and southeastern parts of the island [*Tejada et al.*, 1996a; *Parkinson et al.*, 1996]. The Nd-Pb-Sr isotopic characteristics of the Sigana Basalts closely resemble those at Site 807 and Site 803. Both Unit-A-like (hereafter "A-type") and Units-C-G-like (hereafter "C-G-type") isotopic compositions are present and, as at Site 803, the ≈90 Ma lavas are similar to the C-G-type [*Tejada et al.*, 1996a]. Average incompatible element signatures are again very similar to those at the ODP sites (Figure 6), although a wider range of abundances is present among the Sigana Basalts, including several lavas that appear to be highly differentiated basalts [*Tejada et al.*, 1996a; *Parkinson et al.*, 1996].

In addition to the low-K tholeiitic Sigana Basalts, rare 90 Ma alkalic dikes, termed the Sigana Alkalic Suite [*Tejada et al.*, 1996a], are present within the Sigana Basalt exposures on Santa Isabel. Despite being indistinguishable in age from the younger group of tholeiites, they have high-$^{206}Pb/^{204}Pb$, "HIMU" or "Mangaia Group"-type isotopic signatures quite distinct from those of the tholeiites (Figure 5).

6.3. *Malaita*

6.3.1. *OJP Basement.* Following reconnaissance studies by *Rickwood* [1957] and *Pudsey-Dawson* [1960], *Hughes and Turner* [1976, 1977] mapped the southern part of Malaita, where they termed the basement section the Older Basalts. Recently, the basement lavas throughout the island have been renamed the Malaita Volcanic Group [*Petterson*, 1995]. The ^{40}Ar-^{39}Ar ages of samples collected by Hughes and Turner showed them to be 122 Ma [*Mahoney et al.*, 1993]. All are low-K tholeiites of essentially A-type composition, although rocks from the much more extensive exposures in southern Malaita exhibit somewhat greater chemical and isotopic variation than the 46 m of Unit A flows at Site 807 (e.g., Figure 5) [*Mahoney*, 1987; *Mahoney and Spencer*, 1991; *Tejada et al.*, 1996a].

The thickest exposures of basement crust (reaching 3–4 km in stratigraphic thickness [*Petterson*, 1995; *Tejada et al.*, 1996b; *Petterson et al.*, 1997]) are in the central part of Malaita, which remained unsampled until recently. Basement in central and northern Malaita is exposed in the cores of NW-SE-trending anticlinal to periclinal structures formed in response to the collision of the OJP with the Australian Plate [e.g., *Petterson et al.*, 1997]; the major outcrops of Malaita Volcanic Group rocks are in the Kwaio, Kwara'ae, Fateleka, and Tombaita areas (Figure 7). These areas are dominated by submarine basalt flows which range from <1 m to 60 m in thickness, with most between 4 and 12 m thick; dikes are rare in most locations.

TABLE 1. Compositions of Basalts from Malaita, ODP Leg 130 Sites, and Average Nauru Basin Basalt

	Standard Reference Materials				Malaita			ODP Leg 130			
	BIR-1		BHVO-1		A-Type	C-G-Type	ML475	Site 807	Site 807	Site 803	Nauru
	Publ.	Meas.	Publ.	Meas.	(n=48)	(n=21)		A-Type	C-G-Type		Basin
SiO_2					49.92	49.25	49.68	48.24	49.88	49.09	49.7
TiO_2					1.59	1.20	0.73	1.61	1.15	1.37	1.2
Al_2O_3				14.31	14.47	14.00	14.29	14.24	15.46	13.9	
Fe_2O_3					13.71	12.69	9.84	13.52	12.26	11.59	4.0
MnO					0.20	0.21	0.16	0.20	0.20	0.16	0.2
MgO					7.11	7.75	9.99	6.66	7.64	6.25	6.8
CaO					11.29	12.35	14.52	12.11	12.13	12.22	11.4
Na_2O					2.23	2.05	1.48	2.39	2.20	2.32	2.4
K_2O					0.14	0.14	0.08	0.29	0.15	0.47	0.1
P_2O_5				0.14	0.11	0.06	0.14	0.10	0.15	0.1	
Li	R3.4	3.95	P4.6	4.12	6.42	6.71	3.51				
Be	P0.58	0.14	P1.1	0.97	0.65	0.47	0.25				
K					1139	1129	664.0				
Sc	R44	56.9	R31.8	36.4	44.0	46.5	57.9	46.5	49.3	48.9	47.4
V	R313	476	R317	369	370	314	217	325	347	312	
Cr	R382.0	399.8	R289.0	340.3	96.2	133.0	446.3	156	153	252	245
Co	R51.4	53.7	R45.0	49.2	51.0	50.9	38.8				50.0
Ni	R166	163	R121	119	70.5	98.1	133	96	94	110	115
Cu	R126	113.4	R136	135.7	107.1	140.8	128.0				
Zn	R71	71	R105	106	99	80	47				
Ga	P16.0	15.0	R21.0	25.1	19.4	17.0	13.1				
Rb	I1	.0148	R11	9.93	1.72	1.32	0.91				
Sr	R108	111	R403	425	145	153	135	188	113	172	110
Y	R16	15.7	R27.6	26.4	28.4	22.6	13.5	30.2	25.0	27.6	22.0
Zr	P22	15.9	R179	182	94.1	69.3	29.9	98.6	64.4	79.4	49.5
Nb	P2	0.7	R19	20.3	5.44	3.76	1.57	5.89	3.50	4.45	3
Mo	I0.5	0.10	R1.02	1.004	0.69	0.54	0.18	0.75	0.79	0.50	
Cs	P0.45	0.03	I0.13	0.16	0.02	0.01	0.01	0.19	0.04	0.18	
Ba	P7.7	6.94	R139	135.6	34.1	23.6	11.5	24.1	13.6	16.5	
La	P0.88	0.65	R15.8	15.9	5.59	3.66	1.61	5.79	3.38	4.31	3.4
Ce	I2.5	2.01	R39	40.6	15.72	10.55	4.80	14.39	8.99		9.5
Pr	I0.5	0.35	R5.7	5.22	2.32	1.57	0.72	2.29	1.46	1.78	
Nd	P2.5	2.40	R25.2	25.05	11.64	8.26	3.78	10.79	7.10	8.46	6.3
Sm	R1.1	1.04	R6.2	6.22	3.56	2.67	1.30	3.36	2.39	2.88	2.6
Eu	R0.54	0.51	R2.1	2.11	1.30	0.97	0.51	1.29	0.92	1.11	1.0
Gd	P1.9	1.77	R6.4	6.42	4.46	3.40	1.74	4.31	3.26	3.73	3.3
Tb	R0.41	0.34	R1.0	0.94	0.79	0.62	0.32		0.64	0.73	0.8
Dy	R2.4	2.43	R5.2	5.23	4.93	3.90	2.05	4.94	4.06	4.45	
Ho	P0.5	0.50	I0.99	0.98	1.05	0.83	0.43	1.06	0.90	0.97	
Er	P1.8	1.67	R2.4	2.51	3.01	2.37	1.26	2.99	2.46	2.74	
Tm	P0.27	0.24	R0.33	0.32	0.43	0.34	0.17				
Yb	R1.7	1.60	R2.02	2.07	2.90	2.28	1.16	2.72	2.40	2.59	2.6
Lu	R0.26	0.27	R0.29	0.28	0.43	0.34	0.17	0.41	0.35	0.38	0.4
Hf	R0.58	0.58	R4.38	4.32	2.51	1.91	0.87	2.54	1.65	2.07	1.7
Ta	I0.0006	0.04	R1.23	1.34	0.36	0.27	0.10	0.38	0.21	0.30	0.2
W	I0.20	0.23	P0.27	0.38	0.06	0.04					
Pb	P3.2	3.11	P2	2.04	1.30	0.81	0.40	0.72	0.67		
Th	I0.89	0.02	R1.08	1.23	0.53	0.33	0.12	0.52	0.28	0.35	0.3
U	I0.025	0.027	R0.42	0.43	0.14	0.09	0.03	0.14	0.12	0.21	

Our ongoing work and that of colleagues A. Saunders and T. Babbs (Univ. of Leicester, UK) reveals that broadly C-G-type lavas are present below an A-type cap some 600 m thick ([*Tejada et al.*, 1996b] and C. R. Neal et al.; M. L. Tejada et al.; T. Babbs et al., manuscripts in preparation, 1997). The range of chemical variation is again greater than in the 149 m of flows at Site 807 (Figures 8a–d, 9), but A- and C-G-type basalts can clearly be distinguished in incompatible element (e.g., Figure 6), major element (Figures 8c and 9d), and isotopic (Figure 5) diagrams. Also, all dated basement samples from central Malaita belong to the 122 Ma event [*Tejada et al.*, 1996b]. Thus, no 90 Ma lavas have been found on the island, and A-type lavas form a section more than 13 times thicker than at Site 807, some 1600 km away to the north. The transition between A-type and C-G-type groups is again sharp, but unlike Site 807, where an interlava limestone unit (Unit B) separates the two types, no corresponding sedimentary layer is seen in Malaita. These results suggest that the part of the OJP now exposed on Malaita was more proximal to, or possibly downslope from, the main locus of A-type eruptive activity than Site 807. Moreover, the combined data for Malaita, Santa Isabel, and the drill sites demonstrate that both A- and C-G-type lavas were erupted over a considerable portion of the plateau [cf. *Tejada et al.*, 1996a,b].

For each type, a voluminous, well-mixed mantle source (relative to the scale of melting) is indicated. In the context of a zoned plume-head model, one type may better represent the plume-source composition and the other better reflect average entrained mantle, or the plume source itself may have contained both types; the C-G-type is closer to some estimates of average lower mantle isotopic composition [*Tejada et al.*, 1996a,b]. Intriguingly, lavas of the much more poorly sampled Manihiki Plateau to the east of the OJP (Figure 1) are very close in age to the ≈122 Ma OJP event (R. A. Duncan, unpubl. data, 1993) and also define two isotopic groups, one of which is quite similar to the OJP A-type (Figure 5a,b), possibly suggesting that the sources of the OJP and Manihiki Plateau were related [*Mahoney and Spencer*, 1991; *Mahoney et al.*, 1993]. Indeed, *Coffin and Eldholm* [1993] speculated that the Manihiki Plateau may be part of a "greater" OJP event, along with lavas filling the Nauru and East Mariana basins. Isotopic and elemental data (e.g., Figures 8 and 9) for the basin-filling basalts partially overlap with those for C-G-type OJP lavas [e.g., *Tokuyama and Batiza*, 1986; *Floyd*, 1986; *Castillo et al.*, 1986, 1994; *Saunders*, 1986; *Mahoney*, 1987]. However, their ^{40}Ar-^{39}Ar ages, at 111–115 Ma, are significantly different from either the 122 or 90 Ma events on the OJP, and *Castillo et al.* [1994] proposed that they reflect OJP source mantle that had flowed northward and mixed variably with ambient MORB-type asthenosphere (recall that the OJP itself probably moved very little during this period; see Section 4 and Figure 4).

The similarity in isotopic and incompatible element ratios of the 90 Ma OJP tholeiites to the 122 Ma C-G-type strongly suggests both groups shared a common plume mantle source. As noted above, the plateau may have been located at a roughly similar geographic position at these two times; however, the lack (so far) of any OJP lavas with intermediate ages argues against a smooth plume-head to plume-tail transition after the 122 Ma event. One possibility suggested by simple experimental and theoretical modeling is that the strong bimodality in age of OJP lavas represents a separation of the starting-plume head from its conduit (tail) as it rose through the 660-km mantle discontinuity, followed by formation of a second, smaller head which rose to the base of the lithosphere some 30 m.y. after the first [*Bercovici and Mahoney*, 1994]. Alternatively, plume material may have collected beneath the plateau more or less continuously after 122 Ma, but did not erupt to the surface in significant amounts until a change in the stress field of the OJP around 90 Ma provided the necessary pathways for melt egress [*Tejada et al.*, 1996a; *Ito and Clift*, 1996].

A quite different model was proposed by *Larson and Kincaid* [1996]. They suggested that the 122 Ma event reflected upward advection of a region of the 660-km boundary layer in response to accelerated subduction of slab material into the deep mantle. Ascent of this boundary layer would increase temperatures in the upper mantle above the peridotite solidus and thus cause voluminous plateau magmatism. At about the same time, increased amounts of slab material would encounter the

Note that all Fe is listed as Fe_2O_3. Data for Malaitan basalts from this work, for ODP basalts from *Mahoney et al.* [1993], and the average composition for the Nauru Basin basalts are calculated from *Batiza* [1986], *Tokuyama and Batiza* [1986], *Saunders* [1986], *Castilla et al.* [1986, 1991], and *Floyd* [1986, 1989]. The published compositions of standard reference basalts BIR-1 and BHVO-1 [*Govindaraju*, 1989] are shown along with our ICP-MS (inductively coupled plasma mass-spectrometric) determinations (Meas.) performed during the analyses of the Malaitan basalts. Superscripts on published values: R = recommended values (i.e., most accurately determined abundances); P = provisional abundances; I = data are for information only (least accurately determined abundances). Major element abundances are in wt%; all others are in parts per million.

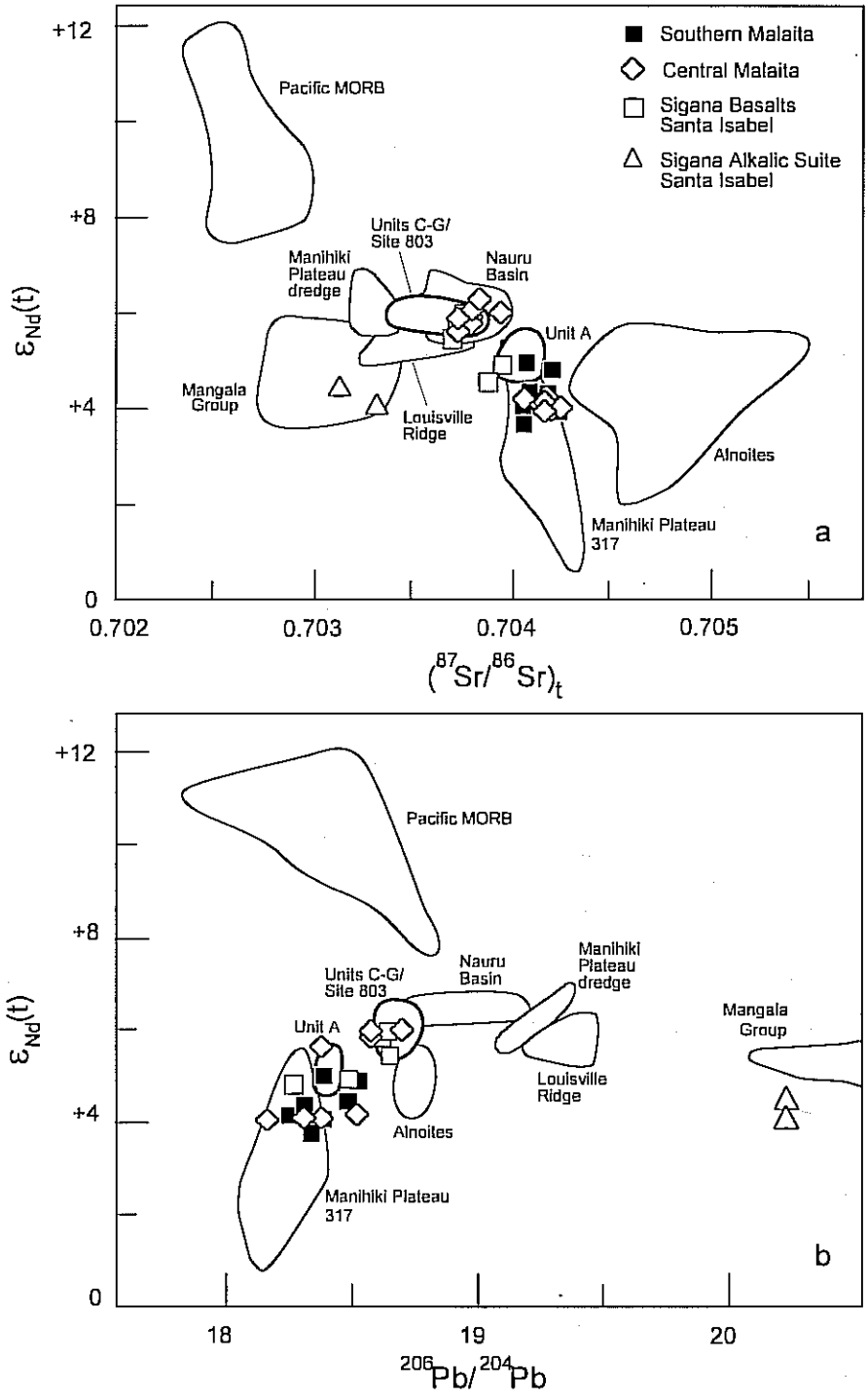

Figure 5. Initial $\varepsilon_{Nd}(t)$ vs. $(^{87}Sr/^{86}Sr)_t$ (a) and present-day $^{206}Pb/^{204}Pb$ (b) for basement lavas of Malaita and Santa Isabel and 90 Ma alkalic dikes of Santa Isabel [*Mahoney*, 1987; *Mahoney and Spencer*, 1991; *Tejada et al.*, 1996a; M. Tejada et al., unpubl. data, 1995]. Fields for A-type and C-G-type/Site 803 drillhole lavas are shown by heavy outlines, those for Malaitan alnöites, Manihiki Plateau, Louisville Ridge, Pacific MORB, and Mangaia Group islands of the South Pacific by light outlines [see *Mahoney et al.*, 1993; *Tejada et al.*, 1996a, for data sources].

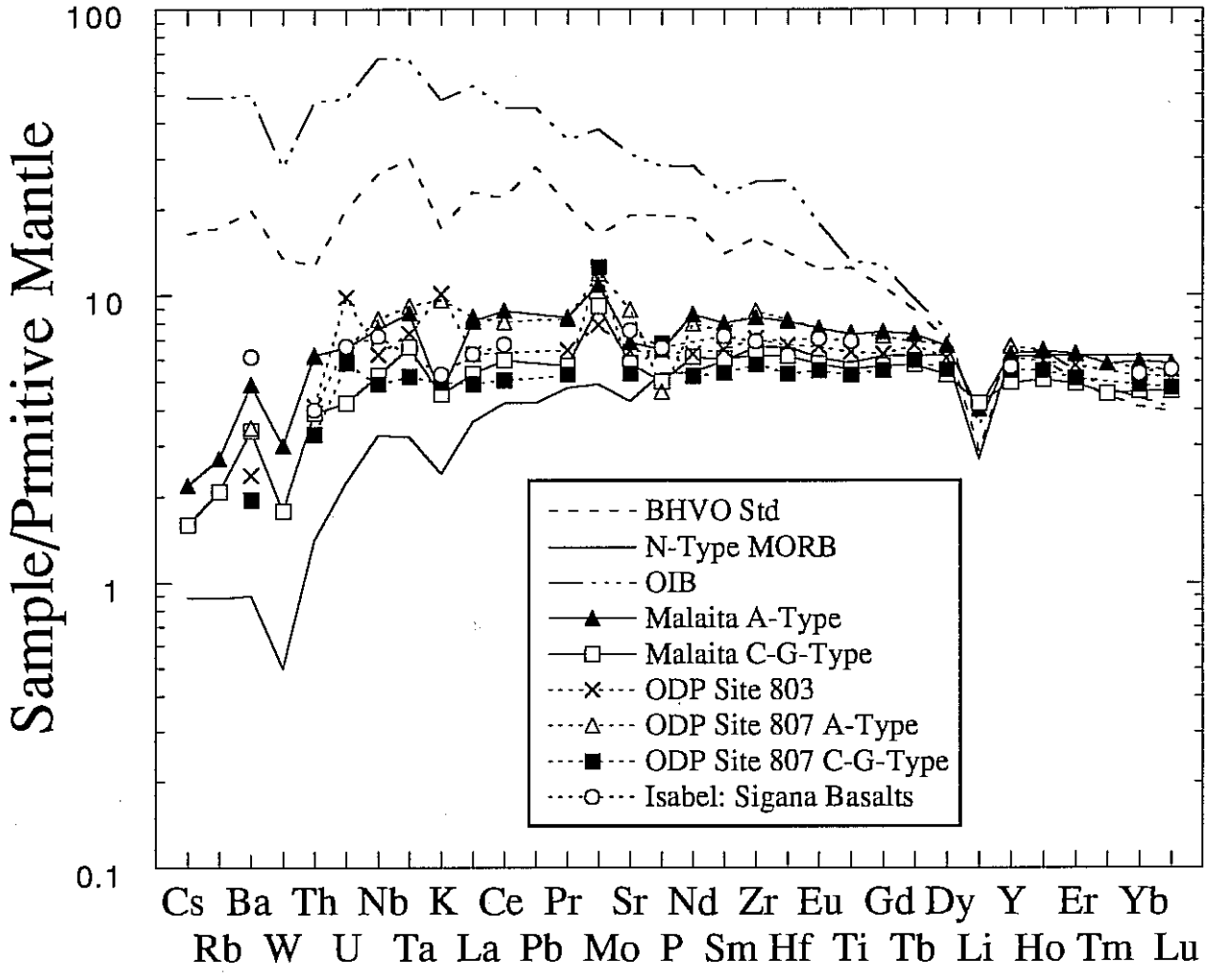

Figure 6. Primitive-mantle-normalized element profiles for average of OJP basalts of Malaita (this study), Sites 803 and 807 [*Mahoney et al.*, 1993], and Santa Isabel [*Tejada et al.*, 1996a]). Average N-type MORB and OIB patterns and primitive-mantle normalizing values are from *Sun and McDonough* [1989]. BHVO-1 standard values are from *Govindaraju* [1989].

core-mantle boundary, and the resulting instability would produce diapiric upwelling argued to reach the surface as a plume head some 20–30 m.y. after the initial magmatic event. This model accounts for the bimodality in the OJP basement ages but implies significant isotopic and chemical differences between the 122 Ma magmatism, which would have an upper mantle and/or 660-km boundary-layer source, and the 90 Ma event, which would have a source originating at the core-mantle boundary. Thus, the model does not explain the marked compositional similarity between the 122 Ma C-G-type and the 90 Ma basalts.

As noted in Section 4, aside from problems associated with pre-90 Ma plate reconstructions, attempts to establish a geochemical link between the OJP and the Louisville hotspot have been unsuccessful. The Nd-Pb-Sr isotopic range defined by ≈70–0 Ma seamount lavas along the ≈4000-km-long Louisville Ridge (see Figure 5) is restricted and values vary little with rock type or age, age of underlying oceanic crust, or depth of melting, indicating a long-lived, isotopically homogeneous source [*Cheng et al.*, 1987; *Hawkins et al.*, 1987]. Although initial ε_{Nd} and $^{87}Sr/^{86}Sr$ values for the Louisville Ridge overlap with those of the 122 and 90 Ma OJP C-G-type basalts (Figure 5), the difference in Pb isotope ratios is substantial (e.g., 0.4 to 1.0 in $^{206}Pb/^{204}Pb$). It is highly unlikely to be the result of radiogenic ingrowth in the plume source between 90 Ma and 70 Ma, but could represent a major compositional

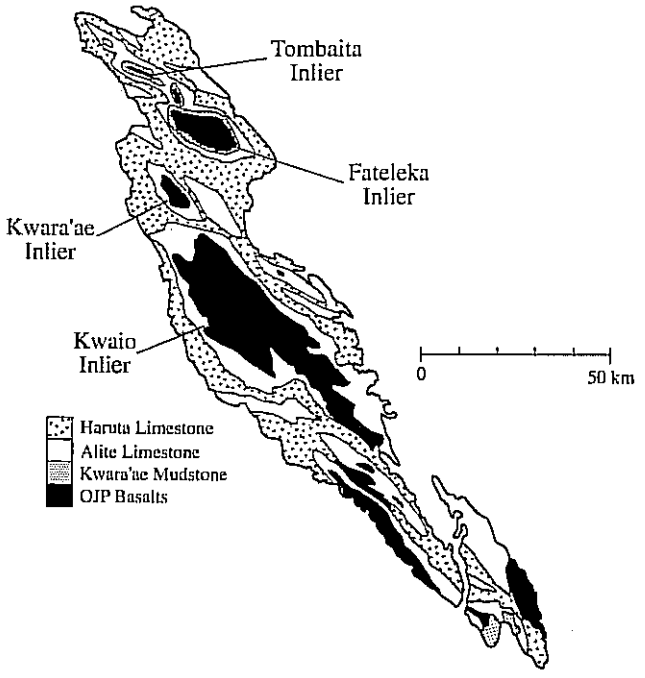

Figure 7. Simplified geological map of Malaita defining the OJP basement inliers [after *Petterson*, 1995].

change from the plume head to plume tail [*Mahoney et al.*, 1993] (as postulated to be a common occurrence by *Campbell and Griffiths* [1990]). Note, however, that the change would have to have occurred during the 20 m.y. period for which the record just happens to be missing [*Mahoney et al.*, 1993].

6.3.2. *Late-Stage Volcanism on Malaita.* Two younger volcanic events are recorded in the pelagic sedimentary section overlying basement on Malaita. The first consists of flows and sills of alkalic basalts cropping out irregularly within Eocene limestones in southern and northern Malaita and the nearby island of Ulawa. Those in southern Malaita were called the Younger Basalts by *Hughes and Turner* [1977], a term superseded by the name Maramasike Volcanic Formation, which includes both the northern and southern exposures [*Petterson*, 1995]. Although they appear at the same stratigraphic level, their thickness varies considerably from place to place, locally reaching a maximum of ≈500 m. An ^{40}Ar-^{39}Ar age of 44.2±0.2 Ma was obtained by *Tejada et al.* [1996a] for one of these basalts. Their Nd-Sr-Pb isotopic ratios are distinct from those of the basement tholeiites, and they may reflect the passage of the OJP over the Samoan hotspot [*Tejada et al.*, 1996a]. Probable counterparts are seen in seismic reflection records of the high plateau north of Malaita, which show numerous sill-like intrusions within the sedimentary section [*Kroenke*, 1972]; moreover, at least some of the large seamounts atop the plateau may be related to Maramasike volcanism.

The second late-stage volcanic event is recorded in central Malaita as several intrusions of alnöite, a rare, ultramafic alkalic magma of deep mantle origin with affinities to kimberlite. With an age of 34 Ma [*Davis*, 1977], the alnöites significantly postdate the Maramasike Volcanic Formation. They appear to correspond to low degrees of melting of sublithospheric mantle [e.g., *Nixon and Boyd*, 1979; *Nixon et al.*, 1980; *Neal*, 1985, 1988] during flexural extension of the OJP as it overrode the outer-trench high prior to colliding with the old North Solomon trench [*Coleman and Kroenke*, 1981; *Petterson*, 1995]. Diatreme-like intrusions, probably correlative with the alnöites on Malaita, are evident in seismic reflection records over about a third of the high plateau [*Kroenke, 1972*; *Nixon*, 1980]. The alnöites contain a rich and varied suite of mantle xenoliths and xenocrysts, which have been studied extensively [e.g., *Nixon and Coleman*, 1978; *Nixon and Boyd*, 1979; *Neal*, 1988, 1995; *Neal and Davidson*, 1989]. Most of the xenoliths appear to represent lithospheric mantle and indicate that this part of the plateau (near the southern edge of the OJP) had a pre-collision lithospheric thickness of about 120 km [*Nixon and Boyd*, 1979]. Isotopically, most of the xenoliths are distinct from the OJP basement tholeiites, with generally higher initial $^{87}Sr/^{86}Sr$ and more variable ε_{Nd} values (Figure 5a) [*Neal*, 1985, 1988; *Neal and Davidson*, 1989], indicating that the lithospheric mantle of the plateau has been variably modified since the plateau formed.

7. EVALUATION OF OJP SOURCE REGION AND MELTING CHARACTERISTICS

7.1. *A Core-Mantle Boundary Origin for the OJP Plume?*

The ultimate origin of the OJP (i.e., the source of the plume) is difficult to evaluate because the presumed plume head arguably contained both plume-source and entrained-mantle components. However, geochemical signatures of the plume source could persist and be detectable in erupted magmas if such signatures were (1) of sufficient magnitude and markedly distinct from those of ambient mantle, and (2) not obliterated by melting or magmatic differentiation processes. Physical considerations imply that plume heads giving rise to the largest LIPs may originate at the core-mantle boundary [e.g., *Campbell and Griffiths*, 1990; *Coffin and Eldholm*, 1991, 1994]. A key chemical "fingerprint" of a core-mantle boundary origin may be the unusual enrichment of siderophilic trace elements [e.g., *Walker et al.*, 1995]; such enrichment may occur by

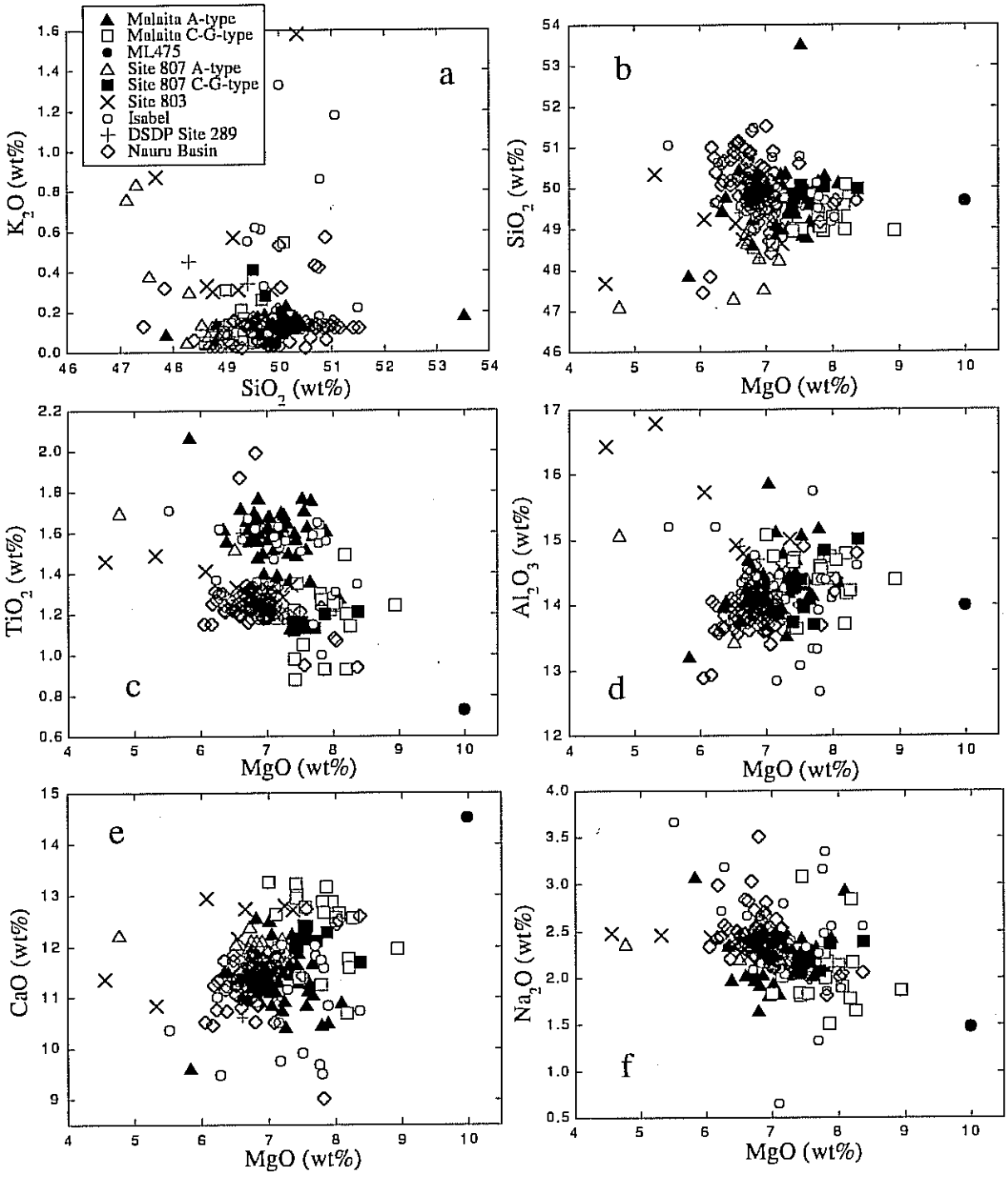

Figure 8. Major element variations in the Malnitan OJP basalts (this study) compared with those of DSDP Site 289 [*Stoeser*, 1975], ODP Leg 130 [*Mahoney et al.*, 1993], Santa Isabel [*Tejada et al.*, 1996a], and the Nauru Basin [*Batiza*, 1986; *Takuyama and Batiza*, 1986; *Saunders*, 1986; *Castillo et al.*, 1986, 1991; *Floyd*, 1986, 1989]. (a) Classification of these basalts generally as low-K tholeiites, with K_2O values > 0.2 wt% probably resulting from low-temperature alteration; (b-f) major element variations using MgO as the fractionation index.

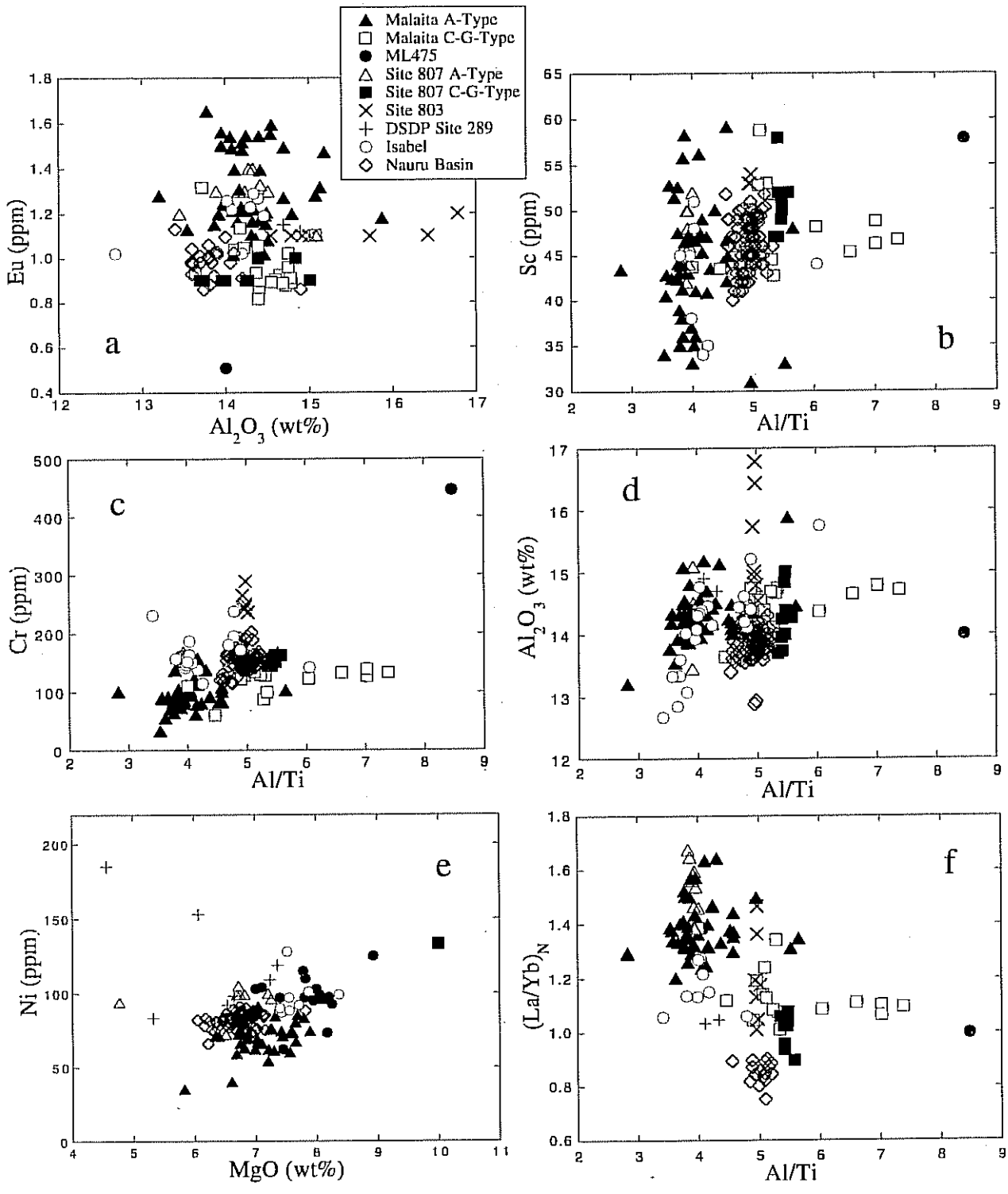

Figure 9. Trace-element comparison of A-type and C-G-type basalts from Malaita with those from Sites 807, 803 and 289, Nauru Basin, and Santa Isabel (data sources as in Figure 8).

entrainment of small amounts of outermost core material during the initial formation of the plume or by chemical diffusion across the boundary [e.g., *Kellogg and King*, 1993]. Unlike major siderophiles (Fe, Ni, Co, etc.), which are affected strongly by silicate melting and differentiation processes, many siderophilic trace elements, such as Mo, W, Au, and Re, as well as those of the platinum group (Rh, Ru, Os, Ir, Pt, Pd), are generally incompatible in silicate minerals [e.g., *Newsom and Palme*, 1984; *Jones and Drake*, 1986; *Fleet et al.*, 1991, 1993; *Walker et al.*, 1993]. Thus, large degrees of partial melting and basaltic-type magmatic differentiation should not significantly alter the ratios of these elements to other incompatible (lithophile) elements.

Jain et al. [1995] reported the presence of a significant enrichment in W and Mo for OJP basalts from the ODP drill sites and Malaita. These ICP-MS data were interpreted as supporting a core-mantle boundary origin for the OJP plume source. However, our recent reanalysis of the samples, using a more aggressive (between-sample) wash procedure [*McGinnis et al.*, 1996, 1997] demonstrates that the W enrichments are an artifact of instrumental memory from previous samples and standards. In fact, the OJP basalts actually exhibit slightly negative anomalies on primitive-mantle-normalized element diagrams (Figure 6), similar to those seen for MORB and ocean island basalts.

In contrast to W, however, a persistent positive Mo anomaly is still evident in primitive-mantle-normalized element patterns (Figure 6). The observed enrichment of Mo in OJP basalts is consistent with a siderophile-element-enriched source region. Preliminary analyses of platinum group elements and Au in OJP basalts also appear consistent with a siderophile-enriched source [e.g., *Jain et al.*, 1996], but more detailed study is required before any definitive statements can be made.

7.2. *Partial Melting of the Plume Head Peridotite Source*

Significant amounts of partial melting of an adiabatically rising plume head should occur when it intersects the peridotite solidus in the upper mantle. One noteworthy characteristic of the OJP basement lavas is illustrated by Figure 10, showing Zr/Nb vs. Zr/Y. These elements would be highly incompatible in the fractionating assemblage (see Section 8.1) and their ratios thus insensitive to different amounts of differentiation. Relative to southern East Pacific Rise MORB, for example, the OJP basalts display a very restricted range of Zr/Nb, consistent with high degrees of partial melting (Nb being highly incompatible and Zr moderately incompatible during melting); however,

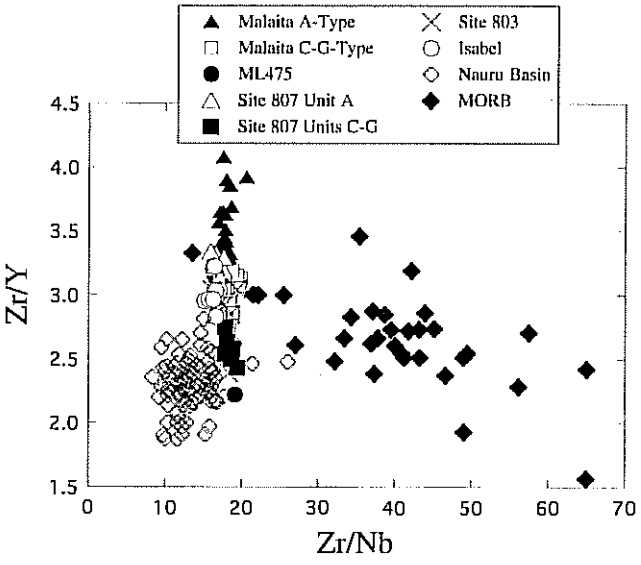

Figure 10. Variations in Zr/Y and Zr/Nb exhibited by the OJP and Nauru Basin basalts (data sources as in Figures 6 and 8) and southern East Pacific Rise MORB [*Mahoney et al.*, 1994].

the Zr/Y ratio varies by nearly a factor of two (Y being moderately incompatible in spinel peridotite but compatible in garnet). Similarly, the variations in Sm/Yb are comparable to those in La/Yb (see Figure 11). These features suggest that melting encompassed both the garnet and spinel peridotite stability fields [cf. *Mahoney et al.*, 1993; *Farnetani et al.*, 1996].

Simple forward modeling can be used to investigate some features of the mantle source and melting process that supplied the A- and C-G-type lavas. Given their generally flat primitive-mantle-normalized element patterns (Figure 6), we took a source with primitive-mantle incompatible element abundances as one possible "end-member". On the other hand, the initial ε_{Nd} values of A-type basalts cluster around +4 to +5, and those of C-G-type lavas around +6 (Figure 5a). These values are roughly halfway between the presumed primitive mantle value of 0 and the average MORB value of about +10, suggesting that a mantle source with mixed elemental characteristics could also be appropriate. For our peridotite source modeling, melting was assumed to initiate in the garnet stability field, with the bulk of melting occurring in the spinel stability field as the plume head impinged on the lithosphere. Initial source mineralogy was estimated from the modal mineralogy of garnet, garnet-spinel, and spinel peridotites studied by *Neal* [1985, 1988] to be 60% olivine, 20% orthopyroxene, 10% clinopyroxene, and 10% garnet, melting in the proportions of 15:30:25:30. After an initial phase of batch or fractional melting in the garnet stability field (minimum of 5%, maximum of 15%), the mode and

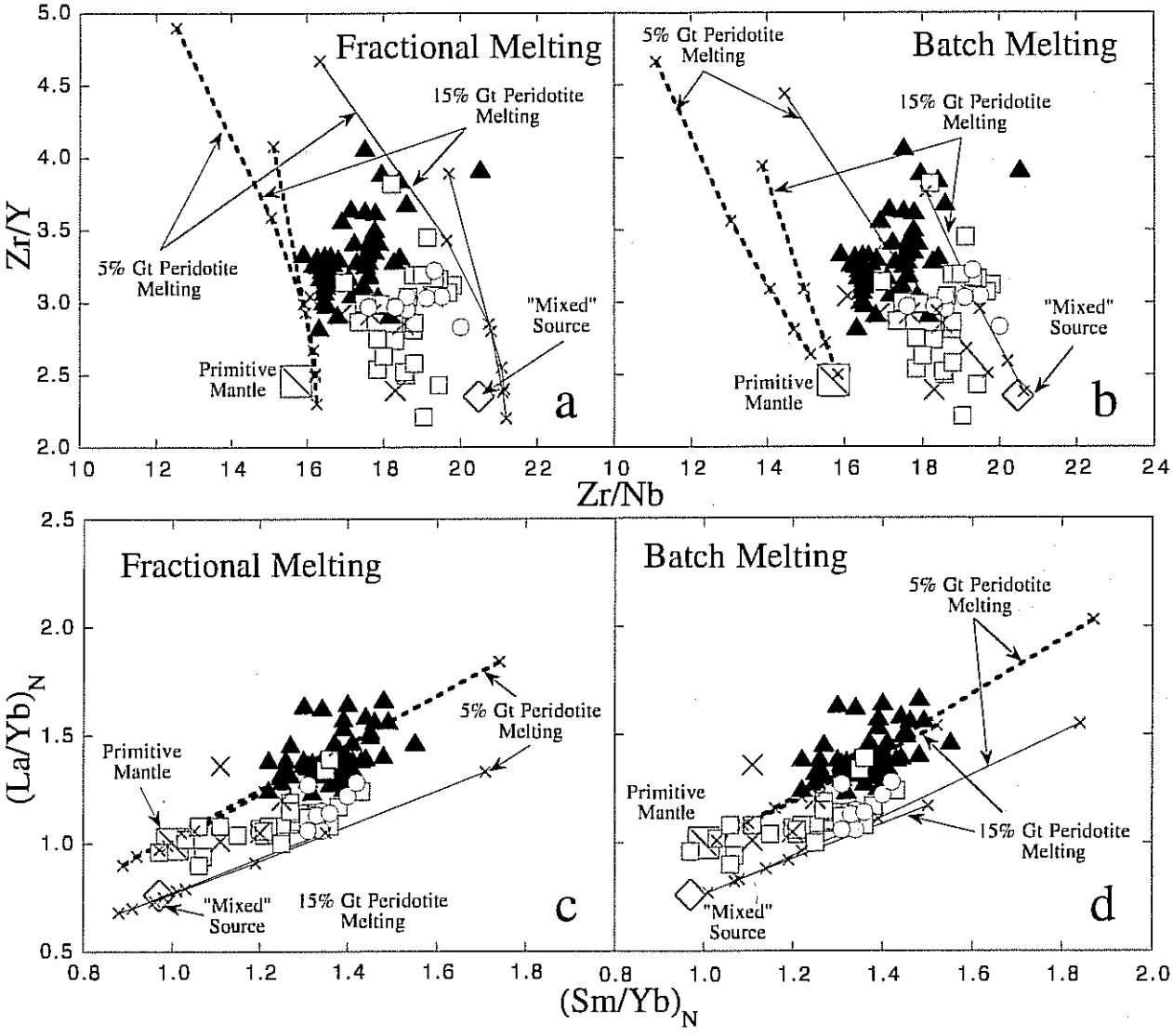

Figure 11. Modeling of trace element ratios as a function of fractional and batch partial melting. The primitive mantle source is taken from *Sun and McDonough* [1989] and the "mixed" source is a 50:50 mixture of primitive mantle and MORB source [*McKenzie and O'Nions*, 1991]. *McKenzie and O'Nions* [1991] reported concentrations for the rare earth elements in their estimated MORB source, but not Zr, Nb, or Y. In estimating concentrations of these elements we assume: (i) a Nb/La ratio of 1, producing a Nb concentration of 0.206 ppm; (ii) a Zr/Nb ratio of 32 which, on the basis of 0.206 ppm Nb, yields a Zr abundance of 6.6 ppm; and (iii) Y abundance is 10 times that of Yb, or 3.47 ppm. The melting trajectories are for hybrid melts, and incorporate melting in both the garnet and spinel peridotite stability fields. Two melting paths are shown for each source: one which incorporates a 5% partial melt and the second a 15% partial melt of the source in the garnet peridotite stability field. To each of these melts are progressively added 5% increments of melt derived from the spinel peridotite stability field after phase transformation facilitated by the rising plume head. The first cross on each melt path (i.e., that farthest from the source composition) represents a 5% or 15% melt from garnet peridotite plus a 5% melt from spinel peridotite, resulting in a minimum partial melt represented on each of these paths of 10% and 20%, respectively. The higher the degree of partial melting, the more the melt composition converges on that of the source. Partition coefficients used are from *Green et al.* [1989] and *Horn et al.* [1994]. Subscript N means chondrite-normalized.

composition of the residue were calculated and subsequent melting was calculated for a spinel peridotite, assuming all remaining garnet was converted to spinel. Melts generated from garnet and spinel peridotite were then mixed to give calculated parental melt compositions. The starting points for the model batch and fractional melting trajectories in Figure 11 represent the minimum- and maximum-degree partial melts generated in the garnet stability field (5% and 15%, respectively) which have been mixed with a 5% melt from spinel peridotite, assuming either a primitive or mixed mantle source (50% MORB source, 50% primitive mantle). The crosses on the trajectories represent mixing, in 5% increments, of these initial compositions with subsequent melts generated in the spinel stability field and formed from the residue of the initial melting. Note that because the later melts are derived from a residue after a phase transformation (and hence a change in bulk partition coefficients) the melt trajectories for neither batch nor fractional melting lead to the initial mantle source compositions as the degree of partial melting is increased.

The partial melting trajectories in Figure 11 imply that the source(s) for the OJP lavas contained a greater proportion of primitive-type mantle than MORB mantle, as the bulk of the data plot between the model trajectories; the model sources and their calculated melt trajectories do, however, generally bracket the basalt data. For simplicity, we have not considered more complicated melting processes (e.g., zone refining) which may have operated to some extent, at least in the garnet peridotite stability field, during the rise of the plume head. From our modeling, the calculated minimum degree of partial melting for the OJP basalts is 15–25% (generally for A-type basalts) and the maximum is 20–35% (generally for C-G-type basalts). However, caution is required in interpreting such melting estimates because these ranges are a product of variation in the model parameters used. The variation is produced by the choice of fractional or batch melting models, the amount of melt derived from the garnet peridotite stability field, and the type of source melted.

The data for A- and C-G-type lavas form two groups with only limited overlap (Figure 11). Although these ranges are small, we believe these groups are real in view of the high precision of the ICP-MS data (errors on individual data points would generally be within the symbol plotted). Given the isotopic differences between the two groups, the small but consistent differences in incompatible element ratios could reflect trace element differences inherent in the respective mantle sources. However, they may also reflect different amounts of partial melting followed by open-system evolution, with the A-type representing lower degrees of melting [cf. *Mahoney et al.*, 1993; *Tejada et al.*, 1996a]. Major elements provide some additional insight. Figure 9d shows the Al/Ti ratio vs. Al_2O_3; despite variable amounts of plagioclase fractionation/accumulation, the OJP basalts exhibit a fairly restricted range in Al_2O_3 (excepting Site 803, the bulk of the samples contain 13.5–14.5 wt%) and again define A- and C-G-type groups in terms of Al/Ti ratio. Changes in Al/Ti will be controlled by the degree of partial melting and, as Al is buffered, decreasing the degree of partial melting will decrease the Al/Ti ratio by increasing the relative abundance of moderately incompatible Ti. Either the individual sources for A-type and C-G-type basalts had distinct mineralogies (not likely from trace element evidence) or the A-type lavas represent a somewhat lower degree of partial melting than the C-G-type basalts.

8. CRYSTAL FRACTIONATION AND THE HIDDEN CUMULATES

8.1. *Fractionation*

Xenoliths are present in some of the 122 Ma C-G-type basement basalts in central Malaita, particularly at deeper stratigraphic levels in the Kwaio inlier. These xenoliths are gabbroic (mainly plagioclase and clinopyroxene, with minor olivine and spinel) and anorthositic. They provide graphic evidence for crystal fractionation, consistent with major-element data for the Malaitan and other OJP basalts, which show that all A-type and C-G-type lavas are evolved; for example, whole-rock molar Mg-number (= $Mg/[Mg+Fe^{2+}]$, assuming that 75% of the total Fe is Fe^{2+}) is 0.50 to 0.29. Preliminary study indicates plagioclase is the predominant phase in the gabbroic xenoliths, whereas the basalt major-element compositions suggest that fractionation of plagioclase was comparatively minor: although Eu may undergo a slight decrease toward the top of the A-type (1.3 ppm → 1.1 ppm) and C-G-type (1.2 ppm →0.9 ppm) portions of the stratigraphic section, Sr is not depleted significantly (e.g., Figure 6), and Al_2O_3 shows a restricted range (most samples have 13.5–14.5 wt%) and does not correlate with Eu or Sr. Plagioclase phenocrysts are fairly common in the lavas, but clinopyroxene is the dominant phenocryst and appears to have been a major fractionating phase. For example, Sc abundances range from 31–59 ppm and Cr contents from 25–200 ppm for A-type and C-G-type (high-MgO sample ML475, with Cr = 446 ppm, exhibits a cumulate texture), with two basalts from Santa Isabel and the 90 Ma samples from Site 803 containing between 200 and 300 ppm Cr (Figure 9b,c). Olivine phenocrysts are rare and MgO-Ni correlations poor, but the generally low Ni contents of the lavas (Figure

9e) indicate olivine was removed, probably as an early fractionating phase. In general, correlations of major elements with typical fractionation indices, such as MgO and Mg-number, are rather poor; in part, this likely reflects a lack of strong olivine control on the analyzed basalts at this evolutionary stage, although effects of seawater-alteration on the lavas and open-system magma plumbing networks [cf. *Mahoney et al.*, 1993; *Tejada et al.*, 1996a,b] cannot be discounted.

As primary OJP magma compositions are unknown, it is difficult to quantify the amount of crystal fractionation; however, estimates can be obtained by combining petrographic and experimental petrologic data. Partial melting appears to have been initiated in the garnet stability field and concluded in the spinel stability field, as discussed above. We estimated the major-element composition of OJP parental magmas by using the experimental results (Table 2) of *Falloon and Green* [1988] for melts derived from garnet peridotite (30 kbar) and *Hirose and Kushiro* [1993] for melts from spinel peridotite (20 kbar). Rather than a single composition, we calculated a range of potential parental compositions assuming 5%, 10%, and 15% partial melting in the garnet stability field, and that the calculated melts then mix with partial melts from the spinel stability field in 5% increments, the total from both fields not exceeding 30% of partial melting (the maximum amount suggested by *Mahoney et al.* [1993] and *Tejada et al.* [1996a]). For example, 5% of garnet peridotite melt mixed with 20% of spinel peridotite melt corresponds to 25% of total melting with a 1:4 proportion of garnet and spinel peridotite end-members. This approach yields picritic melts with high MgO contents averaging 16 wt%.

TABLE 2. Melt Compositions Derived From Garnet- and Spinel-Peridotite Stability Fields and Used in Major Element Modeling

	Garnet Peridotite Melt[1]	Spinel Peridotite Melt[2]
SiO_2	45.83	47.47
TiO_2	1.08	0.75
Al_2O_3	11.70	15.53
Cr_2O_3	0.42	0.21
FeO	9.04	8.51
MgO	19.99	13.94
CaO	10.66	11.11

[1] Melt composition from MYP-90-40 at 35 kbar and 1600°C [from *Falloon and Green*, 1988].

[2] Melt composition from KLB-1 at 20 kbar and 1375°C [from *Hirose and Kushiro*, 1993].

From calculated parental magma compositions corresponding to 15–30% total melting, we modeled a broad crystallization pathway (Figure 12). The liquidus phases used and their relative proportions were derived from petrography (e.g., the range of clinopyroxene and plagioclase compositions used were those measured by electron microprobe for phenocrysts in the Malaita flows; C. R. Neal, unpubl. data, 1995) and experimental petrology (e.g., the known contraction of the olivine and plagioclase liquidus fields and expansion of the pyroxene fields during crystallization of tholeiitic magma under pressure, but <20 kbar [e.g., *Yoder and Tilley*, 1962; *O'Hara and Yoder*, 1967; *BVSP*, 1981]). *Farnetani et al.* [1996] modeled the crystallization of three experimentally derived melts from spinel peridotites under conditions approximating those expected for melts from a plume head. The main crystallizing phases predicted were olivine, clinopyroxene, spinel, plagioclase, and orthopyroxene. With increasing depth of crystallization the cumulate was predicted to change from olivine-orthopyroxene gabbro, through troctolite and/or leucogabbro, to melanogabbro, pyroxenite, or clinopyroxene-norite. In our modeling, five stages of crystallization were assumed, each crystallizing a volume equal to 10% of the starting magma: Stage 1 = 100% olivine (Fo_{90}); Stage 2 = 70% olivine (Fo_{85}) + 30% spinel; Stage 3 = 50% olivine (Fo_{80}), 50% clinopyroxene; Stage 4 = 95% clinopyroxene, 5% plagioclase; Stage 5 = 90% clinopyroxene, 5% plagioclase, 5% orthopyroxene. Figure 12 shows the calculated liquid evolution trends in a plot of MgO/TiO_2 vs. CaO/Al_2O_3 for several different model parental melts; it can be seen that compositions similar to those of most of the OJP basalts are generated primarily during Stage 4 and at the beginning of Stage 5. This result is consistent with the paucity of olivine (and orthopyroxene) phenocrysts in the lavas, and the predominance of clinopyroxene and plagioclase fractionation which has overprinted evidence of the earlier olivine removal (e.g., Figure 9e). The modeling indicates that most OJP lavas result from 30–45% of crystal fractionation and that the xenoliths seen in some flows in central Malaita correspond to relatively late stages of this process (Stage 4 or 5).

8.2. *The Hidden Cumulates*

The cumulate assemblage derived from magmatic evolution similar to that modeled above would consist primarily of early olivine and later clinopyroxene, with lesser amounts of plagioclase, orthopyroxene, and spinel. Corresponding rock types could include dunite, pyroxenite, and gabbro [cf. *Farnetani et al.*, 1996]. An

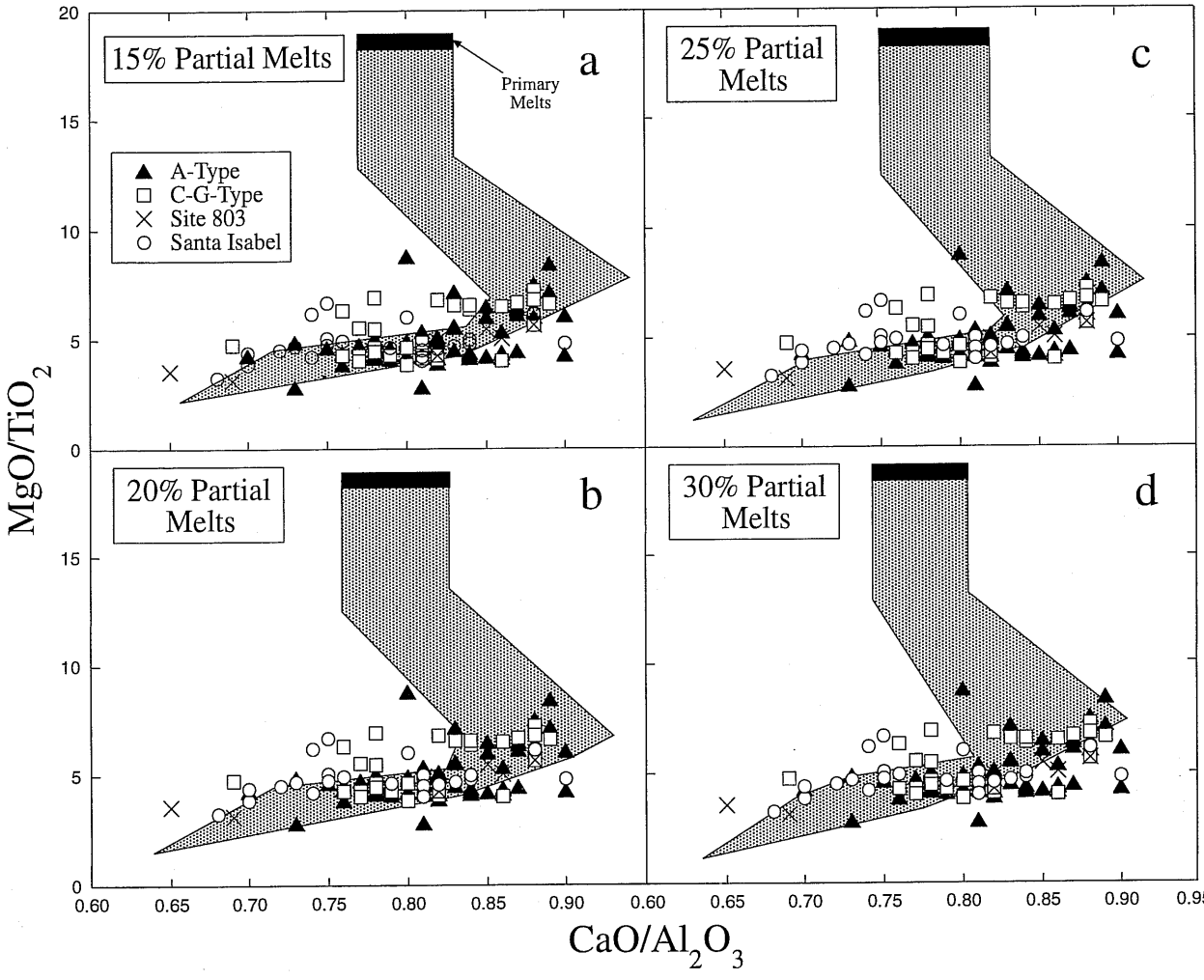

Figure 12. Modeling of the MgO/TiO_2 and CaO/Al_2O_3 variation in OJP basalts by crystal fractionation. Parental melts are estimated from the experimental results of *Falloon and Green* [1988] for melts derived from garnet peridotite (30 kbar) and *Hirose and Kushiro* [1993] for melts from spinel peridotite (20 kbar). These compositions are combined in 5% increments to give the total amount of partial melt at the top of each graph, with the maximum amount of melt from garnet peridotite not exceeding 15% and the resulting parent always being a hybrid of the two melt compositions. Fractional crystallization occurs in five stages, each crystallizing a volume equal to 10% of the starting magma: Stage 1 = 100% olivine (Fo_{90}); Stage 2 = 70% olivine (Fo_{85}) + 30% spinel; Stage 3 = 50% olivine (Fo_{80}), 50% clinopyroxene; Stage 4 = 95% clinopyroxene, 5% plagioclase; Stage 5 = 90% clinopyroxene, 5% plagioclase, 5% orthopyroxene.

MgO content of 30.1 wt% is calculated for the bulk cumulate by using the estimated mean amount of fractionation and corresponding total model fractionating assemblage. Assuming (1) that, as above, the average parental magma MgO = 16 wt%, (2) that the 7.0 wt% average MgO content of OJP samples is representative of erupted liquids on the plateau as a whole, and (3) that the 30.1 wt% MgO value is representative of the bulk cumulate pile, a rough estimate of the total amount of cumulates extracted from the magmas can be made by mass balance [e.g., *Cox*, 1993]:

$$C_P = C_L X_L + C_C X_C$$

where C_P, C_L, and C_C are the concentrations of an element, in this case MgO, in the parental magma, erupted liquid, and cumulate, respectively; and X_L and X_C are the respective mass fractions of erupted liquid and cumulates.

The relative mass of cumulates to erupted liquids is

$$X_C/X_L = (C_L - C_P) / (C_P - C_C)$$

The ratio X_C/X_L gives an estimate of the proportion of crystal cumulates necessary to lower the MgO content of the primary magma from 16.0 wt% to the average 7.0 wt%. Using the above values, the ratio is 0.64; the total, combined fractionating assemblage consists of 49.1% olivine, 40% Ca-rich clinopyroxene, 5.5% spinel, 5.0% plagioclase, and 0.4% orthopyroxene. This assemblage corresponds to a wehrlitic to pyroxenitic cumulate of density ≈3.25 g cm^{-3}. In general agreement, *Cooper et al.* [1986] suggested a density for lower OJP crust of 3.0–3.25 g cm^{-3}, whereas *Gladczenko et al.* [1997] estimated a lower crustal density of 3.25–3.30 g cm^{-3}; both studies utilized gravity data. Conversion of these densities to P-wave velocities (V_P) indicates that the lower OJP crust should exhibit $V_P \geq 7.8$ km s^{-1}, which is not the case (see Figure 2). However, as noted by *Fountain et al.* [1994], reduced average V_P can be obtained by having a heterogeneous lower crust. This may be achieved by the presence of a mixture of gabbro and pyroxenite/wehrlite or basalt and pyroxenite/wehrlite in the lower OJP crust, or their metamorphic derivatives of granulite and possibly eclogite [cf. *Fountain et al.*, 1994].

As discussed earlier, the OJP may partly have formed at a mid-ocean ridge but part, and perhaps much, of the plateau must have been emplaced off-axis. For simplicity, we have taken two extremes: (1) emplacement of the entire plateau at a mid-ocean ridge (no preexisting oceanic crust) and (2) emplacement "off-axis" with a 7.1-km preexisting oceanic crust [*White et al.*, 1992; *Coffin and Eldholm*, 1993]. In addition, minimum and maximum average thicknesses of the OJP are taken as 25 km and 36 km, respectively (see Section 2).

Results of our "hidden cumulate" modeling are as follows. For an off-axis emplacement (presence of a 7.1-km-thick preexisting oceanic crust), cumulate thicknesses vary between 7.0 km (assuming a 25-km total OJP thickness) and 11.3 km (assuming a 36-km total OJP thickness), whereas corresponding erupted basalt sequences would be 10.9 km and 17.6 km, respectively. For an on-axis emplacement (no preexisting oceanic crust), cumulate thicknesses are 9.8 km and 14.0 km, with corresponding basaltic sequences of 15.2 and 22.0 km, respectively. For comparison, recall that the thickness of seismic Layer 2 is estimated at >12 km over much of the high plateau (Figure 2).

Seismic refraction studies of the high plateau identified a basal crustal layer with high P-wave velocity of 7.5–7.7 km s^{-1} (Figure 2) [*Furumoto et al.*, 1976]. The thickness of this seismic layer has been estimated to be 9–16 km [*Furumoto et al.*, 1976; *Hussong et al.*, 1979; *Carlson et al.*, 1981; *Coffin and Eldholm*, 1993]. Over the years, the layer has been ascribed to a variety of possible rock types from, for example, garnet granulites to cumulate gabbros to underplated basalt magma (i.e., non-cumulate gabbros) [*Houtz and Ewing*, 1976; *Nixon and Coleman*, 1978; *Neal and Taylor*, 1989; *Carlson et al.*, 1981; *Schaefer and Neal*, 1994; *Farnetani et al.*, 1996; *Ito and Clift*, 1996]. Compositions between gabbro and pyroxenite would have P-wave velocities between 7.4 and 8.1 km s^{-1} at pressures of ≈10 kbar [e.g., *Carmichael*, 1989]. Therefore, as noted above, mixtures of gabbroic and pyroxenitic cumulates produced by OJP magmatism, or their metamorphic derivatives, are likely to be responsible for much of the basal high-velocity crustal layer.

Significant amounts of intruded and underplated material undoubtedly contribute to the thickness of the OJP [*Tejada et al.*, 1996a; *Ito and Clift*, 1996] as, probably, does some buried preexisting oceanic crust, thus complicating such simple crustal models. Moreover, the relative amounts of magmatism (volcanism, intrusion, and underplating) associated with the 122 and 90 Ma events are unknown and, as noted earlier, the possibility of some magmatism occurring throughout the 30 m.y. period between the two eruptive events cannot be discounted at present. Intrusion and underplating associated with the seamount and Maramasike volcanism on the plateau, possibly caused by the passage of the OJP over the Samoan hotspot (which took place from ≈60–30 Ma [e.g., *Yan and Kroenke*, 1993]), was probably relatively minor but presently is impossible to quantify. A further caveat is that the OJP lavas studied to date represent only the upper levels (≤4 km) of the eruptive section and may not be representative of earlier, deeper levels, which may be more picritic in composition [e.g., *Storey et al.*, 1991].

9. UPLIFT AND SUBSIDENCE OF THE OJP

9.1. *Paleodepths*

The OJP is roughly isostatically compensated [e.g., *Sandwell and MacKenzie*, 1989] and most of it stands 2–3 km above the surrounding seafloor today (although still some 1700 meters or more below sea level). Subsidence rates for normal seafloor of similar age [e.g., *Stein and Stein*, 1992] suggest that the plateau should have subsided some 3 km since its formation. Remarkably, however, although there are indications that the north-central region of the high plateau has subsided a few hundred meters

more than the northeastern margin since the Cretaceous [*Berger et al.*, 1992], little evidence is present for any significant amounts (i.e., >1 km) of post-emplacement subsidence at the locations where basement has been sampled. Rather, normal faults at the northern and eastern margins of the OJP indicate that the adjoining abyssal seafloor in these regions has subsided somewhat relative to the plateau [e.g., *Kroenke*, 1972; DSDP Leg 30 unpubl. reflection profiles; *Kroenke et al.*, 1986; *Hagen et al.*, 1993]. We hypothesize that the less than expected subsidence of the high plateau could reflect (1) partial thermal and magmatic "rejuvenation" at ≈90 Ma and during the OJP's ≈60-30 Ma passage [e.g., *Yan and Kroenke*, 1993] over the Samoan hotspot; (2) the near-neutral buoyancy of the "hidden cumulates" (3.25 g cm^{-3} is generally intermediate between the density of oceanic crust and upper mantle, whether fertile or melt-depleted) that would have fractionated from OJP magmas while the plateau was elevated in response to the physical presence of the plume head (see below); (3) the buoying effect of the melt-depleted (and therefore less dense) upper mantle keel beneath the OJP; and/or (4) the "flexural bulge" of the OJP along the plateau's southwest margin (a response to collision with the Australian Plate [e.g., *Coffin et al.*, 1996]), which would help maintain the elevation of the plateau, at least in this region. Also, *Ito and Clift* [1996] recently suggested that, rather than just a 90 Ma rejuvenation, subsidence may have been tempered by continued underplating of the plateau for ≈30 m.y. between the eruptive events.

If it is assumed for modeling purposes that post-emplacement subsidence of the plateau was, in fact, similar to that of normal oceanic crust, a rough "prediction" of original depth of the OJP's surface can be obtained for each drill site on the plateau. This approach was used to good effect in estimating the uplift associated with the formation of the Kerguelen Plateau [*Coffin*, 1992]. Application to the OJP yields results which are crude but at least generally consistent with emplacement of the basalts well below sea level (e.g., Site 288 = -482 meters, assuming a geophysically determined sediment thickness of 1090 m; Site 803 = -930 meters; Site 807 = -520 meters). However, a large discrepancy exists for Site 289 in that an emplacement of basement above sea level (+202 meters) is indicated, which is in direct contrast with lithological evidence (i.e., bathyal Aptian limestone above basement, lack of evidence for erosional surfaces, lack of vesicularity or oxidation in the basalt recovered, etc.). This indicates that the assumptions used (i.e., sediment and structural conditions at each site reflect regional conditions, complications arising from sediment redeposition and submarine erosion can be ignored, and, most importantly, that subsidence followed the normal seafloor time-depth curve) are not valid in this case. In view of other considerations outlined below, we interpret these results as further evidence that the OJP did not subside as expected of normal oceanic crust. Therefore, these calculations yield only minimum emplacement depths.

Strong evidence for non-emergence of the OJP can be found in the basement lavas in Santa Isabel and Malaita, as well as at the drill sites. Lithological and chemical evidence suggests emplacement near or even below the calcite compensation depth (CCD) in some cases [*Hughes and Turner*, 1977; *Kroenke et al.*, 1991; *Hawkins and Barron*, 1991; *Tarduno*, 1992; *Saunders et al.*, 1993]. Field evidence from the basement sections of Malaita, on the southern flank of the OJP, demonstrates that very little interflow sediment is present; that which exists is siliceous rather than calcareous and the sediments overlying basement are pelagic mudstones, suggesting that emplacement occurred below the ≈122 Ma CCD in this area [*Saunders et al.*, 1993; *Neal et al.*, 1994, 1995]. An Aptian bathyal limestone lies above basement at Site 289 [*Andrews and Packham*, 1975], whereas at Site 807, on the northern flank of the plateau, a thin limestone is intercalated between the A-type and C-G-type basalts, indicating late-stage eruption depth was at least temporarily above the CCD; however, the sediments immediately above basement are not calcareous [*Kroenke et al.*, 1991]. The depth of the CCD during the Cretaceous is poorly known and fluctuated widely, but a rough estimate for 122 Ma is ≈2–3 km [e.g., *Arthur et al.*, 1986]. From CO_2 contents in Site 807 glasses, *Michael and Cornell* [1996] estimated that eruption depths of lavas at this site were in the 1000 m (A-type lavas) to 2500 m (C-G-type) range; note that many of the lavas may have flowed considerable distances from their point of eruption, so that the eruption depth and final emplacement depth may not be the same. However, these depths and the presence of limestones at Sites 807 and 289 may imply that the axis of the OJP plume head, above which maximum dynamic uplift would be expected, was situated closer to the northern end of the high plateau at 122 Ma (i.e., the large, as yet unsampled, domal region of shallower depths to the southwest of Site 289 [cf. *Tejada et al.*, 1996a]). Moreover, because the section of A-type basalts is much thicker at Malaita than at Site 807, the principal site(s) of A-type eruptive activity may not have coincided with the plume axis.

In conclusion, the combination of constructional magmatism and dynamic uplift from impingement of a

plume head was apparently insufficient to raise the basement surface of much of the OJP to shallow depths, although parts may have been shallow, particularly the as yet unsampled crestal regions of the high plateau and eastern salient. This situation contrasts with those for Wrangellia [e.g., *Richards et al.*, 1991; *Lassiter et al.*, 1995] and the Kerguelen Plateau [*Coffin*, 1992], which contain evidence of extensive emergence and subaerial erosion in basal sediment and basalt stratigraphy. However, Wrangellia was built upon an island arc and the Kerguelen Plateau formed in a young, narrow ocean basin and may contain fragments of continental lithosphere [e.g., *Storey et al.*, 1992; *Mahoney et al.*, 1995; *Hassler and Shimizu*, 1995; *Operto and Charvis*, 1996].

9.2. *Estimates of Initial Dynamic Uplift*

Impingement of a plume on the lithosphere will produce temporary surface uplift, even if the plume surfaces beneath a mid-ocean ridge. Rough estimates of the amount of such uplift can be obtained by application of results from experimental and theoretical studies [e.g., *Olson and Nam*, 1986; *Griffiths et al.*, 1989; *Hill*, 1991; *van Keken et al.*, 1993; *Ribe*, 1996]. Such estimates require that the volume of the plume head be known or assumed; some limits on this volume can be obtained from the estimated volume of the plateau and the degree of partial melting involved in producing the basalts.

For modeling purposes, we use a minimum OJP areal value of 1.5×10^6 km^2. (*Coffin and Eldholm* [1994] gave a larger estimate of 1.86×10^6 km^2, including possible OJP-related sequences in the Nauru, East Mariana, and Lyra basins, but here we consider only the plateau itself, as defined by the 4-km depth contour.) A maximum volume of 5.4×10^7 km^3 results from using the maximum estimated average crustal thickness of 36 km, together with the assumption of no preexisting oceanic crust (Section 2). A minimum volume of 2.7×10^7 km^3 is obtained by assuming the OJP formed completely on preexisting oceanic crust and taking the estimated average crustal thickness formed by the OJP plume to be 17.9 km (25 km minus 7.1 km of preexisting crust). Assuming further that all of the OJP formed in the 122 Ma event and that the average degree of partial melting was as low as 15% (typical of values estimated for MORB), then an upper limit on the plume-head volume would be 3.6×10^8 km^3; for a spherical head, this corresponds to a diameter of 883 km. A "pseudominimum" plume-head volume of 9.0×10^7 km^3, with a spherical diameter of 555 km, is obtained hy assuming 30% partial melting and using the lower estimate of OJP volume [cf. *Coffin and Eldholm*, 1993]; of course, if significant amounts of OJP crust formed at 90 Ma, in the 122–90 Ma period, or after 90 Ma, then this minimum estimate would be lower still. Two examples of dynamic uplift modeling are presented below.

9.2.1. *Model 1.* Experiments by *Griffiths et al.* [1989] followed the evolution of surface topography as a buoyant droplet rose through a viscous liquid. Maximum surface uplift was observed when the leading edge of the diapir was 0.2 diapir diameters beneath the surface and was quantified as

$$H_{max} = \frac{0.25(1-\lambda)(\Delta\rho D_o)}{\rho_m}$$

where: H_{max} = maximum uplift; $\lambda = (\rho_m - \rho_l)/(\rho_m - \rho_D)$; ρ_m = upper mantle density (3.3 g cm^{-3}); ρ_l = lithospheric density (3.15 g cm^{-3}); ρ_D = plume head density (varied between 3.1 and 3.15 g cm^{-3} resulting in λ values between 0.75 and 1.0; see Figure 13); $D\rho = \rho_m - \rho_D$; D_o = diameter of spherical plume head.

As expected, the maximum amount of uplift is predicted from the largest plume head (Figure 13). However, this approach implies that maximum dynamic uplift associated with OJP formation would barely exceed 3 km and could be much less.

9.2.2 *Model 2. Hill* [1991] quantified dynamic uplift above a spreading (flattening) plume head and demonstrated that the amount of uplift is sensitive to the initial thermal structure of the overlying material; this is manifested by the temperature difference between the plume head and ambient mantle (DT).

$$E = \alpha \Delta T L$$

Here, E = amount of surface uplift; α = coefficient of thermal expansion (3×10^{-5} °C^{-1}); ΔT = average excess temperature anomaly (in °C); L = thickness of the anomalously hot layer (flattened plume head).

In Figure 14, the same estimates of partial melting and plateau and plume-head volume were used as in Model 1. The difference is that the spherical plume head is considered to have flattened to a disc with a diameter of either 1000, 2000, or 3000 km; the smaller the diameter of the flattened plume head, the greater its thickness and, therefore, the greater the surface uplift. Also included are results from assuming a maximum and minimum ΔT (300 and 100°C, respectively) between plume and ambient mantle. Maximum surface uplift of 4.1 km is obtained for a flattened plume head of minimum diameter, ΔT = 300°C, and partial melting of 15%. If the average degree of partial melting is 20–30%, in the range of values considered most

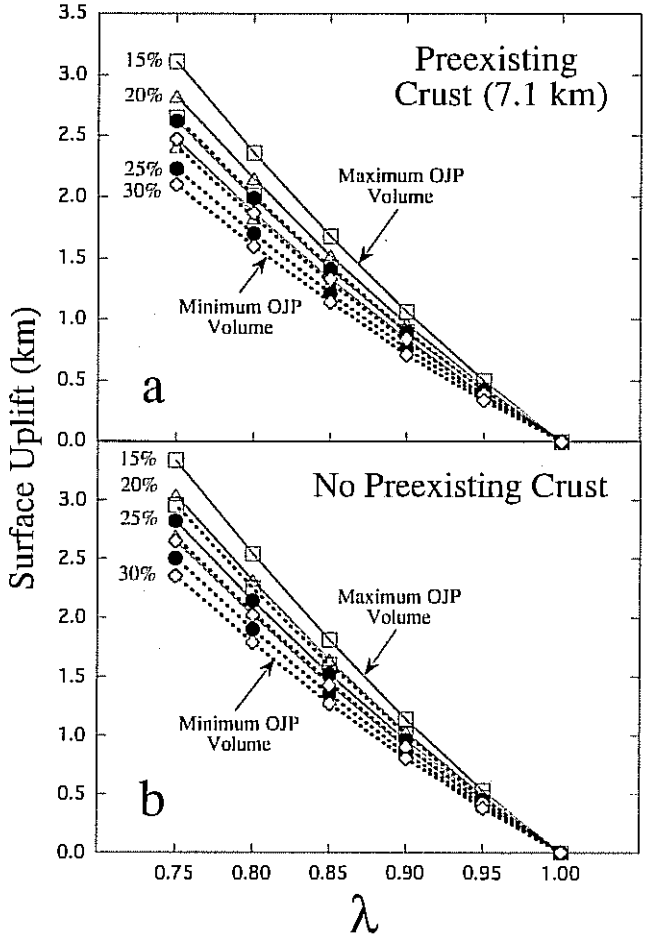

Figure 13. Estimates of surface uplift resulting from impingement of the 122 Ma OJP plume head upon the lithosphere using the model of *Griffiths et al.* [1989]. The maximum volume of the plume head is calculated by assuming a minimum and maximum average thickness of the OJP of 25 and 36 km, respectively. The size of the plume head is directly proportional to the amount of surface uplift. Calculations in (a) assume that the OJP was built upon 7.1 km of preexisting oceanic crust (off-ridge setting), whereas (b) assumes that the total thickness of the OJP was generated by the plume event (ridge setting). Dashed and solid lines represent the minimum and maximum OJP volume, respectively. The percentages represent the assumed amounts of partial melting that generated OJP magmas (i.e., the lower the assumed degree of melting, the larger the plume head required): 15% = open square; 20% = open triangle; 25% = filled circle; 30% = open diamond.

likely for OJP lavas [e.g., *Mahoney et al.*, 1993; *Tejada et al.*, 1996a; Section 7.2, this paper], then the maximum surface uplift would be between 1.0 and 3.0 km, similar to the estimate from the *Griffiths et al.* [1989] approach. (Note that these results are also similar to the minimum uplift values for plateaus estimated by *Farnetani and Richards* [1994], who assumed a greater ΔT (350°C) and a large spherical plume head diameter (800 km)). Again, uplift could be much less.

9.3. *Effect of Added Crust*

Although by itself dynamic uplift appears incapable of raising much of the OJP from ridge or abyssal depths to above sea level, addition of as much as 36 km of new crust might be assumed to cause widespread emergence. However, overwhelming evidence to the contrary is seen at all presently sampled locations. Thus, on average, the bulk density of the OJP must be slightly greater than that of normal ocean crust simply thickened by a factor of up to five or so. For example, mass balance calculations suggest that up to 4 km of surface uplift would result from simply overthickening oceanic crust (density of 2.9 g cm^{-3}). If the density is increased to 3.08 g cm^{-3} (the average density of the OJP we calculate on the basis of P-wave velocities), the surface uplift is reduced to between only 1.8 and 3.0 km, depending upon the thickness assumed for the plateau. Indeed, average crustal densities (estimated from published P-wave velocities [e.g., *Bjarnason et al.*, 1993; *Operto and Charvis*, 1996; *White et al.*, 1996] using the methods of *Bott* [1982]) indicate that bulk crustal density increases from Kerguelen (≈ 2.8 g cm^{-3}) to Iceland (≈ 2.9 g cm^{-3}) to the OJP (≈ 3.1 g cm^{-3}). Although Iceland has an average density greater than that of Kerguelen, it is emergent because of a greater crustal thickness (22–35 km [e.g., *Bjarnason et al.*, 1993; *White et al.*, 1996] vs. 20-25 km [e.g., *Operto and Charvis*, 1996]) and because of the dynamic uplift afforded by the plume beneath the Mid-Atlantic Ridge. Much of the Kerguelen Plateau was also originally at shallow depths or subaerial [*Coffin*, 1992] because of plume-driven dynamic uplift and crustal thickening; as mentioned earlier, it may contain some continental lithospheric material, unlike Iceland.

We conclude that the key to the initial depth of OJP emplacement is largely in the high-velocity basal crustal layer, argued here to have been formed from hidden cumulates plus intruded and underplated gabbros. Also, the extreme thickness of the OJP provides conditions conducive to granulite or, possibly, eclogite development [*Fountain et al.*, 1994; *Rudnick and Jackson*, 1995; *Saunders et al.*, 1996], both of which could contribute to tempering OJP uplift. Mafic granulite xenoliths (including a garnet-bearing variety) are indeed present in the Malaitan alnöites (P. H. Nixon, pers. comm., 1996) at the southern edge of the plateau, and the high P-wave velocities of 8.4–8.6 km/s just below the Moho in the northwestern and

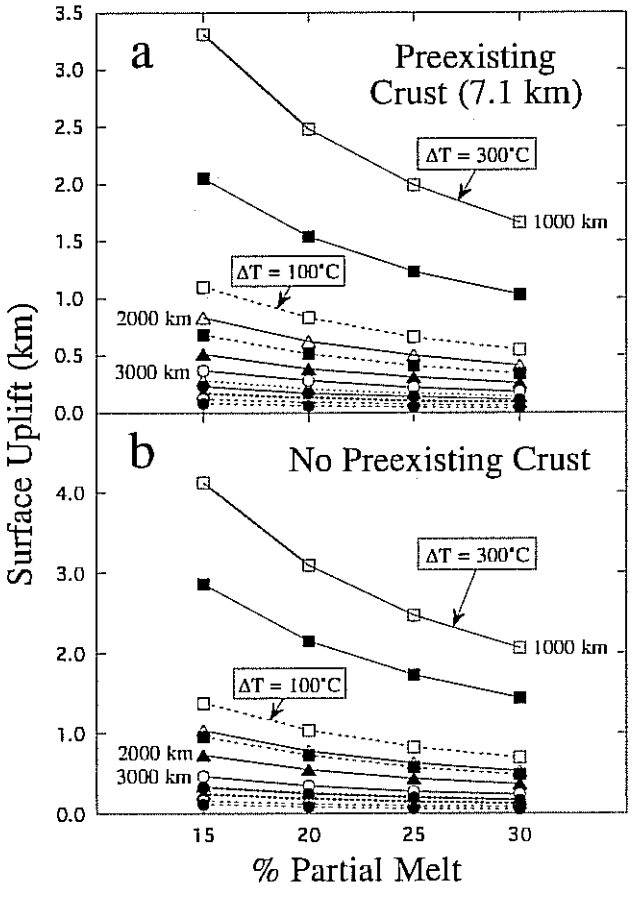

Figure 14. Surface uplift estimated for impingement of the 122 Ma OJP plume head upon the lithosphere using the model of *Hill* [1991] and varying the amount of assumed partial melting between a minimum of 15% and a maximum of 30%. Maximum and minimum plume head sizes are calculated as in Figure 13. Values of ΔT are between the plume head and ambient upper mantle; 100°C is the assumed minimum (dashed lines) and 300°C is the assumed maximum (solid lines). Solid symbols = OJP is 25 km thick; open symbols = OJP is 36 km thick. Assumed flattened plume head diameters: squares = 1000 km; triangles = 2000 km; circles = 3000 km. (a) Assumes that the OJP was built upon 7.1 km of pre-existing oceanic crust (off-ridge setting), whereas (b) assumes that the total thickness of the OJP was generated by the plume event (ridge setting).

southwestern regions of the OJP might represent eclogitized lowermost crust.

9.4. *Melt-Depleted Mantle Root to OJP*

Elevation of the OJP relative to the surrounding ocean floor appears to be persistent as the effects of temporary uplift have long since dissipated. The presence of a relatively dense lower crustal layer beneath much of the high plateau (attributed largely to cumulates) and possible high-density eclogitic material indicated by higher than normal mantle P-wave velocities just below the Moho in parts of the high plateau (see below) would argue for subsidence of the plateau, at least in these areas. In order to maintain plateau elevation and prevent delamination of the high density material, it seems likely that a region of relatively buoyant, melt-depleted mantle resides beneath the plateau, most probably the residue from plateau formation. Degree of partial melting has been estimated from the composition of the OJP basalts to be between 20 and 30% [*Mahoney et al.*, 1993; *Tejada et al.*, 1996a; Section 7.2, this paper]. Such high degrees of partial melting, coupled with the volume of the OJP, require that a significant melt-depleted zone or root be present (barring convective removal) in the upper mantle beneath the plateau. This mantle root would cause a decrease in seismic velocities beneath the OJP and this has indeed been reported recently by *Richardson and Okal* [1996].

An estimate of the depleted mantle root thickness can be made from the mass-balance approach of *Marks and Sandwell* [1991], who used the ratio of geoid height to topography to develop a two-layer (a layer of overthickened crust and a low-density, depleted mantle root) Airy compensation model:

$$(\rho_c-\rho_w)h = (\rho_m-\rho_c)r + (\rho_m-\rho_l)t$$

Here, h = elevation of plateau above the ocean floor (2.5 km); r = thickened layer at the base of the crust, as defined by *Marks and Sandwell* [1991] (taken as thickness of the cumulate layer in our model); t = thickened depleted mantle layer; ρ_c = OJP cumulate density (3.25 g cm^{-3}); ρ_w = seawater density (1.025 g cm^{-3}); ρ_m = mantle density (3.3 g cm^{-3}); ρ_l = melt-depleted mantle density (3.24 g cm^{-3}). The thickness of the depleted mantle layer, t, can be calculated:

$$t = \frac{(\rho_c - \rho_w)}{(\rho_m - \rho_l)}(1-\delta)h$$

The fraction of Airy compensation is represented by δ and corresponds to the compensation associated with the cumulate layer at the base of the OJP. As cumulate thickness depends on the total material added by the OJP plume event(s), r varies between 7 and 14 km (Section 8.2). In order to maintain the mass balance, δ varies between 0.06 and 0.12, respectively. This approach yields a thickness of the melt-depleted mantle of between 82 and 87 km.

As a rough check on the 82- to 87-km root thickness, the average degree of partial melting that created it can be

estimated by dividing the thickness of the OJP crust by the combined thickness of the OJP crust plus depleted mantle root, and the result compared with the degree of partial melting estimated from geochemical evidence. The results imply that the degree of partial melting required to generate the depleted mantle root was between 17% (assuming addition of 17.9 km of material to preexisting 7.1 km thick ocean crust) and 31% (assuming addition of 36 km of crust with no preexisting ocean crust). These values are in excellent agreement with estimates of partial melting from geochemical data [*Mahoney et al.*, 1993; *Tejada et al.*, 1996a; Section 7.2, this paper]. Furthermore, our estimates of the depleted mantle root thickness compare well with the observed region of decreased seismic velocity beneath the OJP [*Richardson and Okal*, 1996; W.P. Richardson, pers. comm., 1996].

10. SUBDUCTIBILITY OF THE OJP

Assuming that subcrustal lithosphere was not compositionally different from surrounding asthenosphere, *Cloos* [1993] concluded from buoyancy analysis that oceanic plateaus >30 km thick would be virtually unsubductible. *Abbott and Mooney* [1995], taking into account the additional buoying effect of a melt-depleted lithospheric mantle root (depleted in both garnet and Fe), argued that oceanic crust thicker than about 25 km should be unsubductible. A critical factor in subductibility is the extent to which density increases when lower parts of a plateau's crust encounter the high pressure region of a subduction zone; the density increase resulting from transformation of lower crust to eclogite can promote subduction of at least the lower portions of plateau crust. *Saunders et al.* [1996] demonstrated that if average OJP crustal thickness is close to 36 km the basal levels of the OJP would be in the eclogite stability field. However, they argued that conversion of lower crust from granulite to eclogite facies would be long-delayed in the absence of small amounts of water (kinetically important for crystal nucleation and transport of ions) and directed stress [e.g., *Austrheim*, 1987]. They suggested that the stress field resulting from arrival of a plateau at a subduction zone and the addition of fluids escaping off a slab subsequently sinking beneath a plateau (following reversal of subduction direction after collision) would promote eclogite formation and cause eventual subduction of at least the lower plateau crust. Ultimately, only those parts of upper crust that had overridden the original forearc (e.g., Malaita, Santa Isabel) might be preserved as identifiable remnants of a plateau.

In the case of the OJP, northeastward subduction began only at 10–5 Ma (see Section 5). Although producing a steeply descending slab beneath the OJP [e.g., *Cooper and Taylor*, 1987], there has been little time for slab-derived fluids to affect more than the edge of the OJP and substantial eclogitization of lower crust by this mechanism has probably not yet occurred (though it may eventually). Nevertheless, *Petterson* [1995], *Mann et al.* [1996], and *Petterson et al.* [1997] have argued that geophysical evidence is consistent with underthrusting of the leading edge of the OJP beneath the Solomon block, even as the upper levels are overriding it. Although superficially resembling true subduction, this process is interpreted by *Petterson et al.* [1997] as a mechanical "wedge effect" of the old forearc splitting the OJP crust and forcing its lower levels downward; as such, it should be of limited magnitude and duration.

Is any significant amount of eclogite present, then, in the OJP? Earlier, we noted that sub-Moho P-wave velocities of 8.4–8.6 km s^{-1} in parts of the high plateau (e.g., Figure 2) might signal the presence of eclogite immediately below the Moho. The regions where these velocities were measured are generally far from the Solomon arc and thus from slab-derived fluids and subduction-related stress. Eclogitization in these (and possibly other) regions, if confirmed by future deep-crustal seismic studies, must have occurred largely in the absence of such factors, following or during emplacement of the plateau's thick crust. Whereas substantial amounts of eclogite could eventually lead to delamination of the plateau's lithosphere in locations far from a subduction zone [e.g., *Saunders et al.*, 1996], the buoying effect of a low-density, melt-depleted root would tend to counteract delamination. For the present, we emphasize that the possibility of an eclogite layer should be considered carefully in future models of OJP structure, subsidence, and eventual fate.

11. FUTURE RESEARCH AVENUES

To evaluate the OJP's origin, history, and consequences more fully, a number of fundamental questions remain to be answered. To a large extent they require (a) a much more comprehensive sampling on and near the OJP of basement and later-stage igneous rocks, and (b) state-of-the-art geophysical studies of the plateau's crustal structure and its relation to surrounding areas. Further detailed sampling is required, for example, to assess the relative contributions of the 122 Ma and 90 Ma events, how much—if any—volcanism occurred in the period between 122 and 90 Ma, and to document how representative the limited range of geochemical variation in the few presently sampled sites is of the plateau's upper crust as a whole. The answers, in turn, would throw light on the size and

composition of the plume head(s) thought to be responsible for the OJP and the relation of plateau emplacement to plate-motion changes. The crests of the high plateau and eastern salient, which may correspond to the locations of the plume axis at 122 and 90 Ma, respectively, are likely to be important for sampling the range of geochemical compositions present. Similarly, drilling in block-faulted areas and possible dipping-reflector sequences [*Kroenke,* 1972] could provide a means of sampling relatively deep into the volcanic pile, possibly even into the upper levels of the cumulate sequence in some places (particularly using a ship with riser capability). Such sampling might well reveal whether early, highly magnesian lavas, predicted to exist in plateau crust and similar to those seen in stratigraphically lower parts of the Caribbean Plateau's eruptive sequence [e.g., *Storey et al.*, 1991; *Kerr et al.*, this volume], are present. Drilling of seismically imaged diatreme-like structures would determine if some are true kimberlites and could yield lower crustal and upper mantle xenoliths similar to those from the Malaitan alnöites, which would be critical for understanding the nature of the lower crust and the refractory/eclogitized upper mantle. Systematic analysis of highly siderophilic trace elements in both future and existing sample collections will be important for testing the hypothesis of a core-mantle boundary origin for the plume source, and for resolving which of the geochemical types seen thus far may better represent the plume source (vs. entrained mantle).

Detailed seismic studies are essential to establish a clearer picture of crustal structure (both upper and lower) and thickness, the composition of the lower crust, as well as the importance of magmatic underplating and the deep-level interaction between the southern OJP and the Solomon block. Coupled with paleodepth data from sediments at sites on and adjacent to the OJP (including the crestal regions of the high plateau and eastern salient, which may have been at relatively shallow levels during emplacement), such information is required for a better understanding of uplift and subsidence history—and of the probability that the OJP will ultimately become accreted to continental crust or at least partially subducted. Evidence is now available that lower crust at the southern edge of the plateau is underthrusting to the southwest [*Mann et al.*, 1996; *Phinney et al.*, 1996; *Cowley et al.*, 1996; *Petterson et al.*, 1997]. Whether this process, which presently appears minor, could evolve into true subduction may depend largely on the extent of lower crustal eclogitization and on the rate at which it may be occurring at present. Future seismic investigations should help evaluate the amount of eclogitization.

Geophysical (including magnetic) studies will also help to decipher the original setting of OJP emplacement, particularly its proximity to a spreading center and which parts of the plateau may have been formed essentially on-axis. Refinement of plate reconstructions for the Early Cretaceous Pacific is needed to better determine the original location of the plateau and its presumed parent plume head.

The global impacts of OJP volcanism on the surface environment, marine and atmospheric chemistry, and the biosphere are very poorly understood at present but may have been significant. For example, widespread early Aptian and early Turonian periods of marine black shale deposition (anoxic events) are well-documented [e.g., *Sliter*, 1989] and may correspond, at least in part, to OJP emplacement. Likewise, excursions in seawater $^{87}Sr/^{86}Sr$ to lower values appear to have occurred in the Aptian and Turonian [*Jones et al.*, 1995]. Moreover, recent research on terrestrial plant fragments and coal seams suggests a sudden increase in atmospheric $^{13}C/^{12}C$ at the beginning of the Aptian that may largely be attributable to OJP volcanism [*Gröcke et al.*, 1997]. In conjunction with dating and geochemical work on OJP basement rocks, further studies of Cretaceous sediments deposited on land, at different depths on pre-OJP edifices in the oceans (the Shatsky Rise, for example), and adjacent to the plateau should help reveal the OJP's role in such environmental changes.

Acknowledgments: Many thanks go to the Ministry of Energy, Water, and Mineral Resources (Geology Mapping) of the Solomon Islands; without their logistical support, constant guidance, diplomacy in the bush, and enthusiasm for field work, this study would not have been possible. Michael Storey, Tadeusz Gladczenko, and co-editor Mike Coffin provided critical reviews which greatly improved this contribution. Thanks also to S. Schaefer, J. Rigert, and J. Westerink for initial direction in cumulate and uplift modeling, and to N. Hulbirt, P. Wessel, and M. Tejada. This study was supported by NSF grants EAR 93-02471 and ECS92-14596 to CRN, EAR 92-19664 to JJM, and EAR 93-02472 to RAD.

REFERENCES

Abbott, D., and W. Mooney, The structural and geochemical evolution of the continental crust: Support for the oceanic plateau model of continental growth, *Rev. Geophys. Suppl.*, US Nat. Rept. to IUGG 1991-1994, 231-242, 1995.

Andrews, J. E., and G. H. Packham et al., *Init. Repts. Deep Sea Drill. Proj., 30*, 753 pp., 1975.

Arthur, M. A., W. E., Dean, and S. O. Schlanger, Variations in the global carbon cycle during the Cretaceous related to climate, volcanism, and changes in atmospheric CO_2, in *The Carbon Cycle and Atmospheric CO_2: Natural Variations Archean to Present. Geophys. Monogr. Ser.*, vol. 32, edited by

E. T. Sundquist and W. S. Broecker, pp. 504-529, AGU Washington, D.C., 1986.

Austrheim, H., Eclogitization of lower crustal granulites by fluid migration through shear zones, *Earth Planet. Sci. Lett., 81*, 221-232, 1987.

Auzende, J-M., L. W. Kroenke, J-Y. Collot, Y. Lafoy, and B. Pelletier, Compressive tectonism along the eastern margin of Malaita island (Solomon Islands), *Mar. Geophys. Res., 18*, 289-304, 1996.

BVSP - Basaltic Volcanism Study Project, *Basaltic Volcanism on the Terrestrial Planets*, 1286 pp., Pergamon Press, 1981.

Batiza, R., Trace-element characteristics of Leg 61 basalts, *Init. Repts. Deep Sea Drill. Proj., 61*, 689-695, 1986.

Bercovici, D., and J. J. Mahoney J. J., Double flood-basalt events and the separation of mantle-plume heads at the 660 km discontinuity, *Science, 266*, 1367-1369, 1994.

Berger, W. H., and T. C. Johnson, Deep sea carbonates: Dissolution and mass wasting on Ontong Java Plateau, *Science, 192*, 785-787, 1976.

Berger, W. H., L. W. Kroenke, L. A. Mayer, J. Backman, T. R. Janacek, L. Krissek, M. Leckie, and M. Lyle, The record of Ontong Java Plateau: Main results of ODP Leg 130, *Geol. Soc. Am. Bull., 104*, 954-972, 1992.

Berger, W. H., R. M. Leckie, T. R. Janacek, R. Stax, and T. Takayama, Neogene carbonate sedimentation on Ontong Java Plateau: Highlights and open questions, *Proc. Ocean Drill. Prog., Sci. Results, 130*, 711-744, 1993.

Birkhold-VanDyke, A. L., C. R. Neal, J. C. Jain, J. J. Mahoney, and R. A. Duncan, Multi-stage growth for the Ontong Java Plateau (OJP)? A progress report from San Cristobal (Makira), Solomon Islands (abstract), *Eos Trans. AGU, 77*, Fall Meeting Suppl., p. 714, 1996.

Bjarnason, I. T., W. Menke, Ó. G. Flóvenz, and D. Caress, Tomographic image of the mid-Atlantic plate boundary in southwestern Iceland, *J. Geophys. Res., 98*, 6607-6622, 1993.

Bott, M. H. P., *The Interior of the Earth: Its Structure, Constitution, and Evolution*, 382 pp., Elsevier, Amsterdam, 1982.

Campbell, I. H., and R. W. Griffiths, Implications of mantle plume structure for the evolution of flood basalts, *Earth Planet. Sci. Lett., 99*, 79-93, 1990.

Cande, S. C., J. L. Labrecque, R. L. Larson, W. C. Pitman III, X. Golovchenko, and W. F. Haxby, *Magnetic Lineations of the World's Ocean Basins (chart)*, American Association of Petroleum Geologists, Tulsa, Okla., 1989.

Carlson, R. L., N. I. Christensen, and R. P. Moore, Anomalous crustal structures in ocean basins: Continental fragments and oceanic plateaus, *Earth Planet. Sci. Lett., 51*, 171-180, 1981.

Carmichael, R. S., *Practical Handbook of Physical Properties of Rocks and Minerals*, 741 pp., CRC Press, Boca Raton, Fla, 1989.

Castillo, P., R. Batiza, and R. J. Stern, Petrology and geochemistry of Nauru Basin igneous complex: large-volume, off-ridge eruptions of MORB-like basalt during the Cretaceous, *Init. Repts. Deep Sea Drill. Proj., 89*, 555-576, 1986.

Castillo, P., R. W. Carlson, and R. Batiza, Origin of the Nauru Basin igneous complex: Sr, Nd, and Pb isotope and REE constraints, *Earth Planet. Sci. Lett., 103*, 200-213, 1991.

Castillo, P., M. S. Pringle, and R. W. Carlson, East Mariana Basin tholeiites: Jurassic ocean crust or Cretaceous rift basalts related to the Ontong Java plume? *Earth Planet. Sci. Lett., 123*, 139-154, 1994.

Cheng, Q., K.-H. Park, J. D. Macdougall, A. Zindler, G. W. Lugmair, J. Hawkins, P. Lonsdale, and H. Staudigel, Isotopic evidence for a hotspot origin of the Louisville seamount chain, in *Seamounts, Islands, and Atolls, Geophys. Monogr. Ser.*, vol. 43, edited by B. Keating, P. Fryer, R. Batiza, and G. Boehlert, pp. 283-296, AGU, Washington, D.C., 1987.

Cloos, M., Lithospheric buoyancy and collisional orogenesis: subduction of oceanic plateaus, continental margins, island arcs, spreading ridges, and seamounts, *Geol. Soc. Am. Bull., 105*, 715-737, 1993.

Coffin, M. F., Emplacement and subsidence of Indian Ridge plateaus and submarine plateaus, in *Synthesis of Results from Scientific Drilling in the Indian Ocean, Geophys. Monogr. Ser.*, vol. 70, edited by R. A. Duncan, D. K. Rea, R. B. Kidd, U. von Rad, and J. K. Weissel, pp. 115-125, AGU, Washington, D.C., 1992.

Coffin, M. F., and O. Eldholm, *Large Igneous Provinces*: JOI/USSAC Workshop Rept. University of Texas at Austin Institute for Geophysics *Tech. Rept. No. 114*, 79 pp., 1991.

Coffin, M. F., and O. Eldholm, Scratching the surface: Estimating the dimensions of large igneous provinces, *Geology, 21*, 515-518, 1993.

Coffin, M. F., and O. Eldholm, Large igneous provinces: crustal structure, dimensions, and external consequences, *Rev. Geophys., 32*, 1-36, 1994.

Coffin, M. F., and L. M. Gahagan, Ontong Java and Kerguelen Plateaux: Cretaceous Icelands? *J. Geol. Soc. Lond., 152*, 1047-1052, 1995.

Coffin, M. F., P. Mann, T. Shipley, E. Phinney, and S. Cowley, Structure and stratigraphy of the southern Ontong Java Plateau (abstract), *Eos Trans. AGU, 77*, Fall Meeting Suppl., p. 712, 1996.

Coleman, P. J., The Solomon Islands as an island arc, *Nature, 211*, 1249-1251, 1966.

Coleman, P. J., A re-evaluation of the Solomon Islands as an arc system, *CCOP/SOPAC Tech. Bull., 2*, 134-140, 1976.

Coleman, P. J., and L. W. Kroenke, Subduction without volcanism in the Solomon Islands arc, *Geo-Mar. Lett., 1*, 129-134, 1981.

Coleman, P. J., and G. H. Packham, The Melanesian borderlands and India-Pacific plates boundary, *Earth Sci. Rev., 12*, 197-233, 1976.

Coleman, P. J., B. McGowran, and R. W. Ramsay, New early Tertiary ages for basal pelagites, northeast Santa Isabel, Solomon Islands (central southwest flank, Ontong Java Plateau), *Bull. Aust. Soc. Explor. Geophys., 9*, 110-114, 1978.

Cooper, P., and B. Taylor, Polarity reversal in the Solomon Islands arc, *Nature, 314*, 428-430, 1985.

Cooper, P., and B. Taylor, The spatial distribution of earthquakes, focal mechanisms, and subducted lithosphere in

the Solomon Islands, in *Marine Geology, Geophysics, and Geochemistry of the Woodlark Basin-Solomon Islands, Circum-Pacific Council far Energy and Mineral Resaurces, Earth Sci. Ser.*, vol. 7, edited by B. Taylor and N. F. Exon, pp. 67-88, Circum-Pacific Council for Energy and Mineral Resources, Houston, Tex., 1987.

Cooper, A. K., M. S. Marlow, and T. R. Bruns, Deep structure of the central and southern Solomon Islands region: Implications for tectonic origin, in *Geology and Offshore Resaurces of Pacific Island Arcs - Central and Western Solomon Islands, Circum-Pacific Cauncil for Energy & Mineral Resaurces, Earth Sci. Ser.*, vol. 4, edited by J. G. Vedder, K. S. Pound, and S. Q. Boundy, pp. 157-175, Circum-Pacific Council for Energy and Mineral Resources, Houston, Tex., 1986.

Cowley, S., P. Mann, M. Coffin, and T. Shipley, Folds and unconformities within the Central Solomons Trough: A record of back-thrusting related to post-Miocene shallow subduction of the Ontong Java Plateau (abstract), *Eos Trans. AGU, 77*, Fall Meeting Suppl., p. 712, 1996.

Cox, K. G., Continental magmatic underplating, *Philos. Trans. R. Soc. Lond., A 342*, 155-166, 1993.

Davis, G. L., The ages and uranium contents of zircon from kimberlites and associated rocks (abstract), *Extended Abstr. 2nd Intl. Kimberlite Conf.*, Santa Fe, 1977.

Duncan, R. A., Radiometric ages from volcanic rocks along the New Hebrides-Samoa lineament, in *Geological Investigations of the Northern Melanesian Borderland, Circum-Pacific Council for Energy and Mineral Resources, Earth Sci. Ser.*, vol. 3, edited by T. M. Brocher, pp. 67-76, Circum-Pacific Council for Energy and Mineral Resources, Houston, Tex., 1985.

Ewing, J., M. Ewing, T. Aitken, and W. J. Ludwig, North Pacific sediment layers measured by seismic profiling, in *The Crust and Upper Mantle of the Pacific Area, Geophys. Monogr. Ser.*, vol. 12, edited by L. Knopoff, C. L. Drake, and P. J. Hart, pp. 147-173, AGU, Washington, D.C., 1968.

Falloon, T. J., and D. H. Green, Anhydrous partial melting of peridotite from 8 to 35 kb and the petrogenesis of MORB, *J. Petrol. Spec. Lithosphere Issue*, pp. 379-414, 1988.

Farnetani, C. G., and M. A. Richards, Numerical investigations of the mantle plume initiation model for flood basalt events, *J. Geophys. Res., 99*, 13,813-13,833, 1994.

Farnetani, C. G., M. A. Richards, and M. S. Ghiorso M. S., Modeling crustal structure in provinces affected by plume volcanism (abstract), *Eos Trans. AGU, 76*, Fall Meeting Suppl., p. 591-592, 1995.

Farnetani, C. G., M. A. Richards, and M. S. Ghiorso, Petrological models of magma evolution and deep crustal structure beneath hotspots and flood basalt provinces, *Earth Planet. Sci. Lett., 143*, 81-96, 1996.

Fleet, M. E., W. E. Stone, and J. H. Crocket, Partitioning of palladium, iridium, and platinum between sulfide liquid and basalt melt: Effects of melt composition, concentration, and oxygen fugacity, *Geochim. Cosmochim. Acta, 55*, 2545-2554, 1991.

Fleet, M. E., S. L. Chryssoulis, W. E. Stone, and C. G. Weisner, Partitioning of platinum-group elements and Au in the Fe-Ni-Cu-S system: Experiments on the fractional crystallization of sulfide melt, *Contrib. Mineral. Petrol., 115*, 36-44, 1993.

Floyd, P. A., Petrology and geochemistry of oceanic intraplate sheet-flow basalts, Nauru Basin, Deep Sea Drilling Project, Leg 89, *Init. Repts. Deep Sea Drill. Proj., 89*, 471-497, 1986.

Floyd, P. A., Geochemical features of intraplate oceanic plateau basalts, in *Magmatism in the Ocean Basins, Spec. Publ. 42*, edited by A. D. Saunders and M. J. Norry, pp. 215-230, The Geological Society, London, 1989.

Fountain, D. M., T. M. Boundy, H. Austrheim, and P. Rey, Eclogite-facies shear zones—deep crustal reflectors? *Tectonophysics, 232*, 411-424, 1994.

Furumoto, A. S., D. M. Hussong, J. F. Campbell, G. H. Sutton, A. Malahoff, J. C. Rose, and G. P. Woollard, Crustal and upper mantle structure of the Solomon Islands as revealed by seismic refraction survey of November-December 1966, *Pac. Sci., 24*, 315-332, 1970.

Furumoto, A. S., J. P. Webb, M. E. Odegard, and D. M. Hussong, Seismic studies on the Ontong Java Plateau, 1970, *Tectonophysics, 34*, 71-90, 1976.

Gladczenko, T. P., M. Coffin, and O. Eldholm, Crustal structure of the Ontong Java Plateau: Modeling of new gravity and existing seismic data, *J. Geophys. Res.*, in revision, 1997.

Govindaraju, K., 1989 compilation of working values and sample description for 272 geostandards, *Geostand. Newsl., 13*, 1-114, 1989.

Green, T. H., S. H. Sie, C. G. Ryan, and D. R. Cousens, Proton microprobe-determined partitioning of Nb, Ta, Zr, Sr, and Y between garnet, clinopyroxene, and basaltic magma at high pressure and temperature, *Chem. Geal., 74*, 201-216, 1989.

Griffiths, R. W., and I. H. Campbell, Stirring and structure in mantle starting plumes, *Earth Planet. Sci. Lett., 99*, 66-78, 1990.

Griffiths, R. W., M. Gurnis, and G. Eitelberg, Holographic measurements of surface topography in laboratory models of mantle hotspots, *Geophys. J., 96*, 477-495, 1989.

Gröcke, D. R., A. Constantine, and M. I. Bird, Palaeo-environmental change recorded in stable carbon-isotopes in Early Cretaceous plant fragments, southeastern Australia, *Aust. J. Botany*, in press, 1997.

Hackman, B. D., The Solomon Islands fractured arc, in *The Western Pacific: Island Arcs, Marginal Seas, Geochemistry*, edited by P. J. Coleman, pp. 179-191, University of Western Australia Press, Nedlands, 1973.

Hagen, R. A., L. A. Mayer, D. C. Mosher, L. W. Kroenke, T. H. Shipley, and E. L. Winterer, Basement structure of the northern Ontong Java Plateau, *Proc. Ocean Drill. Prog., Sci. Results, 130*, 23-31, 1993.

Hammond, S. R., L. W. Kroenke, and F. Theyer, Northward motion of the Ontong Java Plateau between 110 and 30 m.y.: A paleomagnetic investigation of DSDP Site 289. *Init. Repts. Deep Sea Drill. Proj., 30*, 415-418, 1975.

Hassler, D. R., and N. Shimizu, Old peridotite xenoliths from the Kerguelen Islands (abstract), *Eos Trans. AGU, 76*, Fall Meeting Suppl., 693-694, 1995.

Hawkins, M. P., and A. J. M Barron, The geology and mineral

resources of Santa Isabel. Solomon Islands Ministry of Natural Resources, *Geol. Div. Rept. J25*, 114 pp., 1991.

Hawkins, J. W., P. F. Lonsdale, and R. Batiza, Petrologic evolution of the Louisville seamount chain, in *Seamounts, Islands, and Atolls, Geophys. Monogr. Ser.*, vol. 43, edited by P. Fryer, B. Keating, R. Batiza, and G. Boehlert, pp. 235-253, AGU, Washington, D.C., 1987.

Hilde, T. W. C., S. Uyeda, and L. W. Kroenke, Evolution of the western Pacific and its margin, *Tectonophysics, 38*, 145-165, 1977.

Hill, R. I., Starting plumes and continental break-up, *Earth Planet. Sci. Lett., 104*, 398-416, 1991.

Hill, R. I., I. H. Campbell, G. F. Davies, and R. W. Griffiths, Mantle plumes and continental tectonics, *Science, 256*, 186-193, 1992.

Hirose, K., and I. Kushiro, Partial melting of dry peridotites at high pressures: Determination of compositions of melts segregated from peridotite using aggregates of diamond, *Earth Planet. Sci. Lett., 114*, 477-489, 1993.

Hopson, P. M., The geology of east central Santa Isabel. Solomon Islands Ministry of Natural Resources, *Geol. Div. Rept. J23*, 1988.

Horn, I., S. F. Foley, S. E. Jackson, and G. A. Jenner, Experimentally determined partitioning of high field strength and selected transition elements between spinel and basaltic melt, *Chem. Geol., 117*, 193-218, 1994.

Houtz, R. and J. Ewing, Upper crustal structure as a function of plate age, *J. Geophys. Res., 81*, 2490-2498, 1976.

Hughes, G. W., and C. C. Turner, Geology of Southern Malaita, *Honiara Min. Nat. Res. Geol. Survey Div., Bull. No. 2*, 80 pp., 1976.

Hughes, G. W., and C. C. Turner, Upraised Pacific ocean floor, southern Malaita, Solomon Islands, *Geol. Soc. Am. Bull., 88*, 412-424, 1977.

Hussong, D. M., L. K. Wipperman, and L. W. Kroenke, The crustal structure of the Ontong Java and Manihiki oceanic plateaus, *J. Geophys. Res., 84*, 6003-6010, 1979.

Ito, G., and P. Clift, Evidence for multi-staged accretion of the Manihiki and Ontong Java Plateaus from their vertical tectonic histories (abstract), *Eos Trans. AGU, 77*, Fall Meeting Suppl., p. 714, 1996.

Jain, J. C., J. A. O'Neill Jr., C. R. Neal, J. J. Mahoney, and M. G. Petterson, Siderophile elements in large igneous provinces (LIPs): Origin of the Ontong Java Plateau at the core-mantle boundary? (abstract), *Eos Trans. AGU, 76*, Fall Meeting Suppl., p. 700, 1995.

Jain, J. C., C. R. Neal, J. A. O'Neill Jr., and J. J. Mahoney, Origin of the Ontong Java Plateau (OJP) at the core-mantle boundary: Platinum group element (PGE) and gold (Au) evidence (abstract), *Eos Trans. AGU, 77*, Fall Meeting Suppl., p. 714, 1996.

Jones, C. E., H. C. Jenkyns, A. L. Coe, and S. P Hesselbo, Strontium isotopic variations in Jurassic and Cretaceous seawater, *Geochim. Cosmochim. Acta, 58*, 3061-3075, 1995.

Jones, J. H., and M. J. Drake, Geochemical constraints on core formation in the Earth, *Nature, 322*, 221-228, 1986.

Kellogg, L. H., and S. D. King, Effect of mantle plumes on the growth of D" by reaction between the core and mantle, *Geophys. Res. Lett., 20*, 379-382, 1993.

Kent, R. W., M. Storey, and A. D. Saunders, Large igneous provinces: Sites of plume impact or plume incubation? *Geology, 20*, 891-894, 1992.

Kincaid, C., D. W. Sparks, and R. Detrick, The relative importance of plate-driven and buoyancy-driven flow at mid-ocean ridges, *J. Geophys. Res., 101*, 16,177-16,193, 1996.

Kroenke, L. W., Geology of the Ontong Java Plateau, *Hawaii Inst. Geophys. Rept., HIG-72-5*, 119 pp., 1972.

Kroenke, L. W., and J. J. Mahoney, Rifting of the Ontong Java Plateau's eastern salient and seafloor spreading in the Ellice Basin: Relation to the 90 Myr eruptive episode on the plateau (abstract), *Eos Trans. AGU, 77*, Fall Meeting Suppl., p. 713, 1996

Kroenke, L. W., and W. Sager, The formation of oceanic plateaus on the Pacific Plate (abstract), *Eos Trans. AGU, 74*, Fall Meeting Suppl., p. 555, 1993.

Kroenke, L. W., and P. Wessel, Pacific plate motion between 125 and 90 Ma and the formation of the Ontong Java Plateau (abstract), *Chapman Conf. on Global Plate Motions*, Marshall, CA, 1997.

Kroenke, L. W., R. Moberly Jr., and G. R. Heath, Lithologic interpretation of continuous reflection profiling, Deep Sea Drilling Project, Leg 7, *Init. Repts. Deep Sea Drill. Proj., 7*, 1161-1227, 1971.

Kroenke, L. W., J. Resig, and P.A. Cooper, Tectonics of the southeastern Solomon Islands: Formation of the Malaita Anticlinorium, in *Geology and Offshore Resources of Pacific Island Arcs—Central and Western Solomon Islands, Earth Sci. Ser.*, vol. 4, edited by J. G. Vedder, K. S. Pound, and S. Q. Boundy, pp. 109-116, Circum-Pacific Council for Energy and Mineral Resources, Houston, Tex., 1986.

Kroenke, L. W., W. Berger,, T. R. Janacek, et al., *Proc. Ocean Drill. Prog., Init. Repts. 130*, 1240 pp., 1991.

Kroenke, L. W., W. Berger, and Leg 130 Shipboard Scientific Party, *Proc. Ocean Drill. Prog., Sci. Results, 130*, 867 pp., 1993.

Larson, R. L., and C. Kincaid, Onset of mid-Cretaceous volcanism by elevation of the 670 km thermal boundary layer, *Geology, 24*, 551-554, 1996.

Lassiter, J. C., D. J. DePaolo, and J. J. Mahoney, Geochemistry of the Wrangellia flood basalt province: Implications for the role of continental and oceanic lithosphere in flood basalt genesis, *J. Petrol., 36*, 983-997, 1995.

Mahoney, J. J., An isotopic survey of Pacific oceanic plateaus: Implications for their nature origin, in *Seamounts, Islands, and Atalls, Geophys. Monogr. Ser.*, vol. *43*, edited by B. Keating, P. Fryer, R. Batiza, and G. Boehlert, pp. 207-220, AGU, Washington, D.C., 1987.

Mahoney, J. J., and K. J. Spencer, Isotopic evidence for the origin of the Manihiki and Ontong Java oceanic plateaus, *Earth Planet. Sci. Lett., 104*, 196-210, 1991.

Mahoney, J. J., W. B. Jones, F. A. Frey, V. J. M. Salters, D. G. Pyle, and H. L. Davies, Geochemical characteristics of lavas from Broken Ridge, the Naturaliste Plateau, and southernmost

Kerguelen Plateau: Cretaceous plateau volcanism in the southeast Indian Ocean, *Chem. Geol., 120*, 315-345, 1995.

Mahoney, J. J., J. M. Sinton, M. D. Kurz, J. D. Macdougall, K. J. Spencer, and G. W. Lugmair, Isotope and trace element characteristics of a super-fast spreading ridge: East Pacific Rise, 13-23°S, *Earth Planet. Sci. Lett., 121*, 173-193, 1994.

Mahoney, J. J., M. Storey, R. A. Duncan, K. J. Spencer, and M. Pringle, Geochemistry and age of the Ontong Java Plateau, in *The Mesozoic Pacific: Geology, Tectonics, and Volcanism, Geophys. Monogr. Ser.*, vol. 77, edited by M. S. Pringle, W. W. Sager, W. V. Sliter, and S. Stein, pp. 233-262, AGU, Washington, D.C., 1993.

Mammerickx, J., and S. M. Smith, Bathymetry of the north-central Pacific, *Map and Chart Series MC-52*, The Geological Society of America, Boulder, Colo. 1985.

Mann, P., L. Gahagan, M. Coffin, T. Shipley, S. Cowley, and E. Phinney, Regional tectonic effects resulting from the progressive East-to-West collision of the Ontong Java Plateau with the Melanesian Arc System (abstract), *Eos Trans. AGU, 77*, Fall Meeting Suppl., p. 712, 1996.

Marks, K. M., and D. T. Sandwell, Analysis of geoid height versus topography for oceanic plateaus and swells using nonbiased linear regression, *J. Geophys. Res., 96*, 8045-8055, 1991.

Mayer, L. A., and J. A. Tarduno, Paleomagnetic investigation of the igneous sequence, Site 807, Ontong Java Plateau, and a discussion of Pacific true polar wander, *Proc. Ocean Drill. Prog., Sci. Results, 130*, 51-59, 1993.

Mayer, L. A., T. H. Shipley, E. L. Winterer, D. Mosher, and R. A. Hagen, Seabeam and seismic reflection surveys on the Ontong Java Plateau, *Proc. Ocean Drill. Prog., Sci. Results, 130*, 45-75, 1991.

McGinnis, C. E., C. R. Neal, and J. C. Jain, Development of an analytical technique for the accurate & precise determination of the high field strength elements (HFSEs), Cs, & Mo by ICP-MS with geological applications (abstract), *Eos Trans. AGU, 77*, Fall Meeting Suppl., p. 772, 1996.

McGinnis, C. E., C. R. Neal, and J. C. Jain, Analytical technique for the accurate and precise determination of the high field strength elements (HFSEs) by ICP-MS with geological applications, *Geostand. Newsl.*, in revision, 1997.

McKenzie, D., and R. K. O'Nions, Partial melt distributions from inversion of rare earth element concentrations, *J. Petrol., 32*, 1021-1091, 1991.

Michael, P. J., and W. C. Cornell, H_2O, CO_2, Cl, and S contents in 122 Ma glasses from Ontong Java Plateau, ODP 807C: Implications for mantle and crustal processes (abstract), *Eos Trans. AGU, 77*, Fall Meeting Suppl., p. 714, 1996.

Miura, S., M. Shinohara, N. Takahashi, E. Araki, A. Taira, K. Suyehiro, M. Coffin, T. Shipley, and P. Mann, OBS crustal structure of Ontong Java Plateau converging into Solomon Island arc (abstract), *Eos Trans. AGU, 77*, Fall Meeting Suppl., p. 713, 1996.

Murauchi, S., W. J. Ludwig, N. Den, H. Hotta, T. Asanuma, T. Yoshi, A. Kubotera, and K. Hagiwara, Seismic refraction measurements on the Ontong Java Plateau northeast of New Ireland, *J. Geophys. Res., 78*, 8653-8663, 1973.

Nakanishi, M., and E. L. Winterer, Tectonic events of the Pacific Plate related to the formation of the Ontong Java Plateau (abstract), *Eos Trans. AGU, 77*, Fall Meeting Suppl., p. 713, 1996.

Nakanishi, M., K. Tamaki, and K. Kobayashi, Magnetic anomaly lineations from late Jurassic to early Cretaceous in the west-central Pacific Ocean, *Geophys. J. Int., 109*, 701-719, 1992.

Neal, C. R., Mantle studies in the western Pacific and kimberlite-type intrusives, Unpubl. Ph.D. Thesis, University of Leeds, UK, 365 pp., 1985.

Neal, C. R., The origin and composition of metasomatic fluids and amphiboles beneath Malaita, Solomon Islands, *J. Petrol., 29*, 149-179, 1988.

Neal, C. R., The relationship between megacrysts and their host magma and identification of the mantle source region (abstract), *Eos Trans. AGU, 76*, Fall Meeting Suppl., p. 664, 1995.

Neal, C. R., and J. P. Davidson, An unmetasomatized source for the Malaitan alnöite (Solomon Islands): Petrogenesis involving zone refining, megacryst fractionation, and assimilation of oceanic lithosphere, *Geochim. Cosmochim. Acta, 53*, 1975-1990, 1989.

Neal, C. R., and L. A. Taylor, Negative Ce anomaly in a peridotite xenolith from Malaita, Solomon Islands: Evidence for crustal recycling into the mantle or mantle metasomatism?, *Geochim. Cosmochim. Acta, 53*, 1035-1040, 1989.

Neal, C. R., J. J. Mahoney, A. D. Saunders, and T. L. Babbs, Trace element characteristics of a 3.5-4 km thick section of OJP basalts, Malaita, Solomon Islands (abstract), *Eos Trans. AGU, 75*, Fall Meeting Suppl., p. 727, 1994.

Neal, C. R., S. Schaefer, J. J. Mahoney, and M. G. Petterson, Uplift associated with large igneous province (LIP) petrogenesis: A case study of the Ontong Java Plateau, SW Pacific (abstract), *Abstracts with Programs, 27 No. 6, Geol. Soc. Am.*, p. A48, 1995.

Neavel, K. E., and A. M. Johnson, Entrainment in compositionally buoyant plumes, *Tectonophysics, 200*, 1-15, 1991.

Newsom, H. E., and M. J. Palme, The depletion of siderophile elements in the Earth's mantle: New evidence from molybdenum and tungsten, *Earth Planet. Sci. Lett., 69*, 354-364, 1984.

Nixon, P. H., Kimberlites in the south-west Pacific, *Nature 287*, 718-720, 1980.

Nixon, P. H., and F. R. Boyd, Garnet-bearing lherzolites and discrete nodule suites from the Malaita alnöite, Solomon Islands, SW Pacific, and their bearing on oceanic mantle composition and geotherm, in *The Mantle Sample: Inclusions in Kimberlites and Other Volcanics*, edited by F. R. Boyd and H. O. A. Meyer, pp. 400-423, AGU, Washington, D.C., 1979.

Nixon, P. H., and P. J. Coleman, Garnet-bearing lherzolites and discrete nodule suites from the Malaita alnöite, Solomon Islands, and their bearing on the nature and origin of the Ontong Java Plateau, *Bull. Aust. Soc. Explor. Geophys., 9*, 103-106, 1978.

Nixon, P. H., R. H. Mitchell, and N. W. Rogers, Petrogenesis of alnöitic rocks from Malaita, Solomon Islands, Melanesia, *Mineral. Mag., 43*, 587-596, 1980.

O'Hara, M. J., and H. S. Yoder Jr., Formation and fractionation of basic magmas at high pressures, *Scott. J. Geol., 3*, 67-117, 1967

Olson, P., and H. A. Singer, Creeping plumes, *J. Fluid Mech., 158*, 511-531, 1985.

Olson, P., and I. S. Nam, Formation of seafloor swells by mantle plumes, *J. Geophys. Res., 91*, 7181-7191, 1986.

Operto, S., and P. Charvis, Deep structure of the southern Kerguelen Plateau (southern Indian Ocean) from ocean bottom seismometer wide-angle seismic data, *J. Geophys. Res., 101*, 25,077-25,103, 1996.

Parkinson, I. J., R. J. Arculus, E. McPherson, and R. A. Duncan, Geochemistry, tectonics and the peridotites of the northeastern Solomon Islands (abstract), *Eos Trans. AGU, 76*, Fall Meeting Suppl., p. 642, 1996.

Petterson, M. G., The geology of north and central Malaita, Solomon Islands (including implications of geological research on Makira, Savo Island, Guadalcanal, and Choiseul between 1992 & 1995), *Geological Mem., 1/95*, Water and Mineral Resources Division, Ministry of Energy, Water, and Mineral Resources, Honiara, Solomon Islands, 1995.

Petterson, M. G., C. R. Neal, A. D. Saunders, T. L. Babbs, J. J. Mahoney, and R. A. Duncan, Speculations regarding the evolution of the Ontong Java Plateau (abstract), *Eos Trans. AGU, 76*, Fall Meeting Suppl., p. 693, 1995.

Petterson, M. G., C. R. Neal, J. J. Mahoney, L. W. Kroenke, A. D. Saunders, T. L. Babbs, R. A. Duncan, D. Tolia, B. McGrail, and M. Barron, Structure and deformation of north and central Malaita, Solomon Islands: Tectonic implications for the Ontong Java Plateau - Solomon arc collision and for the fate of oceanic plateaus, *Tectonophysics*, in revision, 1997.

Phinney, E., P. Mann, M. Coffin, and T. Shipley, Along-strike variations in the style of oceanic plateau accretion within the Malaita accretionary prism, Solomon Islands (abstract), *Eos Trans. AGU, 77*, Fall Meeting Suppl., p. 712, 1996.

Pringle, M. S., J. D. Obradovich, and R. A. Duncan, Estimated ages for magnetic anomaly M0 and interval ISEA, and a minimum estimate for the duration of the Aptian (abstract), *Eos Trans. AGU, 73*, Fall Meeting Suppl., p. 633, 1992.

Pudsey-Dawson, P.A., South Malaita geological reconnaisances, 1957-1958, *British Solomon Islands Geol. Rec., 1957-1958*, 27-31, 1960.

Ramsay, W. R. H., Crustal strain phenomena in the Solomon Islands: Constraints from field evidence and the relationship to the India-Pacific plates boundary, *Tectonaphyics, 87*, 109-126, 1982.

Ribe, N. M., The dynamics of plume-ridge interaction 2. Off-ridge plumes, *J. Geophys. Res., 101*, 16,195-16,204, 1996.

Ribe, N. M., U. R. Christensen, and J. Theißing, The dynamics of plume-ridge interaction, 1: Ridge-centered plumes, *Earth Planet. Sci. Lett., 134*, 155-168, 1995.

Richards, M. A., R. A. Duncan, and V. E. Courtillot, Flood basalts and hot-spot tracks: Plume heads and tails, *Science, 246*, 103-107, 1989.

Richards, M. A., D. L. Jones, R. A. Duncan, and D. J. DePaolo, A mantle plume initiation model for the Wrangellia flood basalt and other oceanic plateaus, *Science, 254*, 263-267, 1991.

Richardson, W. P., and E. Okal, Crustal and upper mantle structure of the Ontong Java Plateau from surface waves: Results from the Micronesian PASSCAL experiment (abstract), *Eos Trans. AGU, 77*, Fall Meeting Suppl., p. 713, 1996.

Rickwood, F. K., Geology of the island of Malaita, in *Geological Reconnaissance of Parts of the Central Islands of the B.S.I.P.: Colonial Geol. and Min. Res., 6*, 300-306, 1957.

Rudnick, R. L., and I. Jackson, Measured and calculated elastic wave speeds in partially equilibrated mafic granulite xenoliths: Implications for the properties of an underplated lower continental crust, *J. Geophys. Res. 100*, 10,211-10,218, 1995.

Sager, W. W., and H.-C. Han, Rapid formation of the Shatsky Rise oceanic plateau inferred from its magnetic anomaly, *Nature, 364*, 610-613, 1993.

Sandwell, D. T., and K. R. MacKenzie, Geoid height versus topography for oceanic plateaus and swells, *J. Geophys. Res., 84*, 7403-7418, 1989.

Sandwell, D. T., and M. L. Renkin, Compensation of swells and plateaus in the North Pacific: No direct evidence for mantle convection, *J. Geophys. Res., 93*, 2775-2783, 1988.

Saunders, A. D., Geochemistry of basalts from the Nauru Basin, Deep Sea Drilling Project Legs 61 and 89, *Init. Repts. Deep Sea Drill. Proj., 89*, 499-518, 1986.

Saunders, A. D., M. Storey, R. W. Kent, and M. J. Norry, Consequences of plume-lithosphere interactions, in *Magmatism and the Causes of Continental Break-Up, Spec. Publ. 68*, edited by B. C. Storey, T. Alabaster, and R. J. Pankhurst, pp. 41-59, The Geological Society, London, 1992.

Saunders, A. D., T. L. Babbs, M. J. Norry, M. G. Petterson, B. A. McGrail, J. J. Mahoney, and C. R. Neal, Depth of emplacement of oceanic plateau basaltic lavas, Ontong Java Plateau and Malaita, Solomon Islands: Implications for the formation of oceanic LIPs? (abstract), *Eos Trans. AGU, 74*, Fall Meeting Suppl., p. 552, 1993.

Saunders, A. D., J. Tarney, A. C. Kerr, and R. W. Kent, The formation and fate of large oceanic igneous provinces, *Lithos, 37*, 81-89, 1996.

Schaefer, S., and C. R. Neal, An estimate of uplift associated with the Ontong Java Plateau and the importance of cumulates (abstract), *Eos Trans. AGU, 75*, Fall Meeting Suppl., p. 711, 1994.

Sliter, W. V., Aptian anoxia in the Pacific Basin, *Geology, 17*, 909-912, 1989.

Sliter, W. V., and R. M. Leckie, Cretaceous planktonic foraminifers and depositional environments from the Ontong Java Plateau with emphasis on Sites 803 and 807, *Proc. Ocean Drill. Prog., Sci. Results, 130*, 63-84, 1993.

Smith, W. H. F., and D. T Sandwell, Oceanographic "pseudogravity" in marine gravity fields derived from declassified Geosat and ERS-1 altimetry (abstract), *Eos Trans. AGU, 76*, Fall Meeting Suppl., p. 151, 1995a.

Smith, W. H. F., and D. T. Sandwell, Marine gravity field from declassified Geosat and ERS-1 altimetry (abstract), *Eos Trans. AGU, 76*, Fall Meeting Suppl., p. 152, 1995b.

Stein, C. A., and S. Stein, A model for the global variation in

oceanic depth and heat flow with lithospheric age, *Nature, 359*, 123-129, 1992.

Steiner, M. B., and B. P. Wallick, Jurassic to Paleocene paleolatitudes of the Pacific Plate derived from the paleomagnetism of the sedimentary sequences at Sites 800, 801, and 802, *Proc. Ocean Drill. Prog., Sci. Results, 129*, 431-446, 1992.

Stoeser, D. B., Igneous rocks from Leg 30 of the Deep Sea Drilling Project, *Init. Repts. Deep Sea Drill. Proj., 30*, 410-444, 1975.

Storey, M., J. J. Mahoney, L. W. Kroenke, and A. D. Saunders, Are oceanic plateaus sites of komatiite formation? *Geology, 19*, 376-379, 1991.

Storey, M., R. Kent, A. D. Saunders, V. J. Salters, J. Hergt, H. Whitechurch, J. H. Sevigny, M. F. Thirlwall, P. Leat, N C. Ghose, and M. Gifford, Lower Cretaceous volcanic rocks along continental margins and their relationship to the Kerguelen Plateau, *Proc. Ocean Drill. Prog., Sci. Results, 120*, 33-54, 1992.

Sun, S.-s., and W. F. McDonough, Chemical and isotopic systematics of oceanic basalts: Implications for mantle composition and processes, in *Magmatism in the Ocean Basins, Spec. Publ. 42*, edited by A. D. Saunders and M. J. Norry, pp. 313-345, Geological Society of London, 1989.

Tarduno, J. A., Vertical and horizontal tectonics of the Cretaceous Ontong Java Plateau (abstract), *Eos Trans. AGU, 73*, Fall Meeting Suppl., p. 532, 1992.

Tarduno, J. A., and W. W. Sager, Polar standstill of the mid-Cretaceous Pacific plate and its geodynamic Implications, *Science, 269*, 5226-5228, 1995.

Tarduno, J. A., W. V. Sliter, L. W. Kroenke, M. Leckie, J. J. Mahoney, R. J. Musgrave, M. Storey, and E. L. Winterer, Rapid formation of the Ontong Java Plateau by Aptian mantle plume volcanism, *Science, 254*, 399-403, 1991.

Taylor, B., Mesozoic magnetic anomalies in the Lyra Basin (abstract), *Eos Trans. AGU, 59*, Fall Meeting Suppl., p. 320, 1978.

Taylor, S. R., *Planetary Science: A Lunar Perspective*, 481 pp., Lunar and Planetary Institute, Houston, Tex., 1982.

Tejada, M. L. G., J. J. Mahoney, R. A. Duncan, and M. P. Hawkins, Age and geochemistry of basement and alkalic rocks of Malaita and Santa Isabel, Solomon Islands, southern margin of the Ontong Java Plateau, *J. Petrol., 37*, 361-394, 1996a.

Tejada, M. L. G., J. J. Mahoney, R. A. Duncan, and C. R. Neal, Geochemistry and age of the Ontong Java Plateau (OJP) crust in central Malaita, Solomon Islands (abstract), *Eos Trans. AGU, 77*, Fall Meeting Suppl., p. 715, 1996b.

Tokuyama, H., and R. Batiza, Chemical composition of igneous rocks and origin of the sill and pillow basalt complex of Nauru Basin, Southwest Pacific, *Init. Repts. Deep Sea Drill. Proj., 61*, 673-687, 1986.

van Keken, P. E., D. A. Yuen, and A. P. van den Berg, The effects of shallow rheological boundaries in the upper mantle on inducing shorter time scales of diapiric flows, *Geophys. Res. Lett., 20*, 1927-1930, 1993.

Walker, D., L. Norby, and J. H. Jones, Superheating effects on metal-silicate partitioning of siderophile elements, *Science, 262*, 1858-1861, 1993.

Walker, R. J., J. W. Morgan, and M. F. Horan, ^{187}Os enrichment in some plumes: Evidence for core-mantle interaction? *Science, 269*, 819-822, 1995.

Wessel, P., and L. W. Kroenke, Relocating Pacific hotspots and refining absolute plate motions using a new geometric technique, *Nature*, in press, 1997.

White, R. S., J. H. McBride, P. K. H. Maguire, B. Brandsdóttir, W. Menke, T. A. Minshull, K. R. Richardson, J. R. Smallwood, R. K. Staples, and the FIRE Working Group, Seismic images of crust beneath Iceland contribute to long-standing debate, *Eos Trans. AGU, 77*, 197-201, 1996.

White, R. S., D. McKenzie, and R. K. O'Nions, Oceanic crustal thickness from seismic measurements and rare earth element inversions, *J. Geophys. Res., 97*, 19,683-19,715, 1992.

Whitehead, J. A., and D. S. Luther, Dynamics of laboratory diapir and plume models, *J. Geophys. Res., 80*, 705-717, 1975.

Winterer, E. L., Bathymetry and regional tectonic setting of the Line Islands chain, *Init. Repts. Deep Sea Drill. Proj., 33*, 731-748, 1976.

Winterer, E. L., and M. Nakanishi, Evidence for a plume-augmented, abandoned spreading center on Ontong Java Plateau (abstract), *Eos Trans. AGU, 76*, Fall Meeting Suppl., p. 617, 1995.

Yan, C. Y., and L. W. Kroenke, A plate-tectonic reconstruction of the southwest Pacific, 100-0 Ma, *Proc. Ocean Drill. Prog., Sci. Results, 130*, 697-710, 1993.

Yoder, H. S., Jr., and C. E. Tilley, Origin of basalt magmas: An experimental study of natural and synthetic rock systems, *J. Petrol., 3*, 342-532, 1962.

R. A. Duncan, College of Oceanic and Atmospheric Sciences, Ocean Administration Building 104, Oregon State University, Corvallis, OR 97331.

L. W. Kroenke and J. J. Mahoney, School of Ocean and Earth Science and Technology, University of Hawaii, Honolulu, HI 96822.

C. R. Neal, Department of Civil Engineering and Geological Sciences, University of Notre Dame, Notre Dame, IN 46556.

M. G. Petterson, British Geological Survey, Murchison House, West Mains Road, Edinburgh, EH9 3LA, United Kingdom.